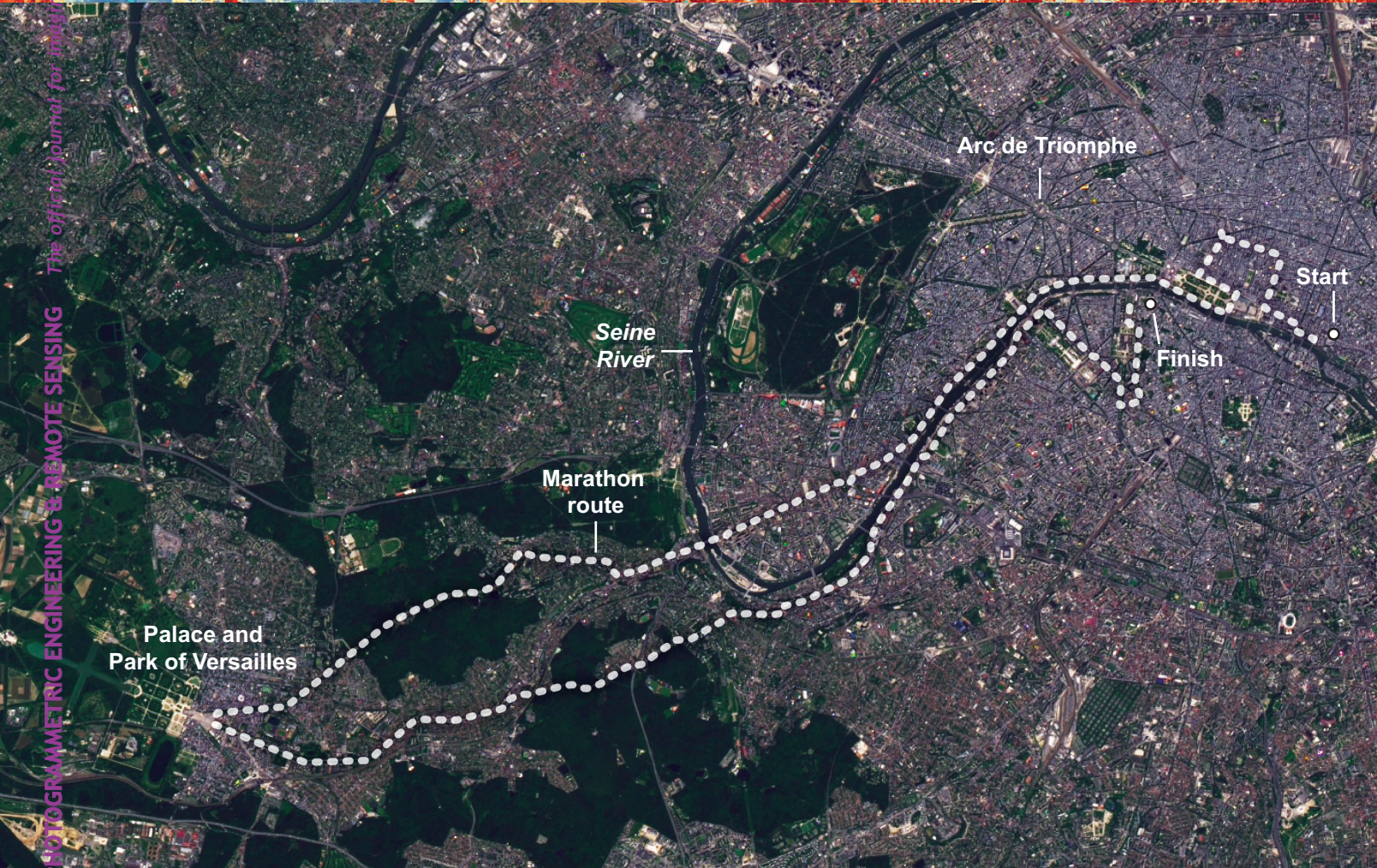


PE&RS

October 2024

Volume 90, Number 10



The official journal for imaging and remote sensing in photogrammetry, engineering and technology

PHOTOGRAMMETRIC ENGINEERING & REMOTE SENSING



Joining ASPRS is a great way to boost your resume and learn valuable life lessons

WHY GET INVOLVED WITH ASPRS?

- Develop leadership skills
- Experience working on a team
- Gain valuable soft skills
- Network
- Learn about yourself
- Have fun!

Scholarships

The many ASPRS scholarships are only available to student members

Certification

The ASPRS certification program for mapping scientists, photogrammetrists and technologists is the only fully Accredited certification program in the geospatial sciences

Continuing Education

Earn professional development hours and CEUs by attending workshops at our conferences and on-line as well as our monthly on-line geobytes series


PE&RS


Our monthly journal, is packed with informative and timely articles designed to keep you abreast of current developments in your field. Now available in e-format.

Get Connected

 facebook.com/ASPRS.org

 linkedin.com/company/asprs/about/

 twitter.com/ASPRSorg

 youtube.com/user/ASPRS

*Image and text courtesy
the ASPRS Florida Region*

ANNOUNCEMENTS

Seamless Integration of Xer X8 UAV and TrueView 720 for Precision 3D Imaging. **GeoCue**, <https://geocue.com/>, and Xer Technologies AG, a Swiss manufacturer of long-endurance hybrid-electric drones, have successfully integrated GeoCue's TrueView 720 LiDAR and imagery sensor with the Xer X8 UAV platform. This collaboration marks a significant advancement in scalable long-range LiDAR and imagery drone mapping technology.

The combination of the long-range, heavy-payload Xer X8 and the GeoCue TrueView 720 enhances aerial operations, enabling high-quality point cloud and imagery data collection over vast and challenging terrains. The integration significantly improves the aerial mapping and inspection workflow by delivering precise and reliable data, allowing operators to manage and monitor large areas more effectively.

"The integration of the Xer X8 UAV and GeoCue's TrueView 720 sensor opens new possibilities for our clients, enabling them to create point clouds, digital twins, and maps over extended distances with unparalleled accuracy and speed," said Gökmen Çetin, International Sales Manager at Xer Technologies. "This partnership demonstrates our commitment to providing innovative solutions that meet the industry's evolving needs."

"GeoCue is pleased to partner with Xer Technologies to bring this advanced 3D imaging solution to market," said Vincent Legrand, Vice President Global Sales at GeoCue. "The Xer X8 drone, combined with our TrueView 720 sensor, offers an outstanding platform for collecting high-quality lidar and imagery data, enhancing the capabilities and productivity of professionals worldwide."

This collaboration highlights both companies' commitment to advancing lidar and UAV technology, delivering efficient and scalable solutions for a wide range of lidar applications.



Windward Risk Managers, the company that manages Florida Peninsula Insurance, Edison Insurance, and the newly formed Ovation Home Insurance Exchange, has signed a multi-year agreement with **Vexcel Data Program**, <https://vexceldata.com>, securing an enterprise license to access high-resolution aerial imagery and post-disaster damage assessments on properties. This partnership will enhance Windward's claims operations by providing vital insights before and after natural disasters, helping the company better serve its customers, estimate damages, and triage response teams.

Both researchers and NOAA predict an above-normal hurricane season for 2024, and Windward is getting ready to

respond faster and more effectively at scale with high-resolution aerial imagery and accurate damage assessments.

Vexcel deploys its fleet of fixed-wing aircraft equipped with photogrammetric sensors to collect post-disaster imagery (called Gray Sky) of impacted areas after hurricanes, tornadoes, and wildfires. Vexcel rapidly processes and publishes the detailed imagery to help insurers, government agencies, and others understand the full scope of the disaster. In addition, by using the latest in AI and machine learning, Vexcel provides a damage assessment of every property in the Gray Sky collection area that includes an overall CAT score, roof damage score, and more.

Windward Risk Managers will use this detailed aerial imagery and property-level damage assessments for its future hurricane claims response to better manage resources, understand exactly which customers have been impacted and at what level, and more accurately estimate the overall loss. By streamlining claims operations and prioritizing resources, Windward can accelerate claims closure, enabling policyholders to begin the rebuilding process sooner.

"In addition to better managing resources and more accurately estimating the ultimate loss, we look forward to being more proactive in serving our customers who experience hurricane damage now that we have Vexcel," said Mike Williams, Senior VP of Claims and Litigation at Windward Risk Managers.



The Sanborn Map Company Inc. (Sanborn), <https://sanborn.com/>, has advanced its geophysical survey and mapping services by equipping its aircraft fleet with state-of-the-art geophysical survey technology developed and produced by the company. In addition to wingtip pods and a tail "stinger" that houses a sensitive magnetometer, inside the plane are a gamma ray spectrometer and data acquisition system, enabling the capture of detailed subsurface data crucial for mapping geological structures and natural resources.

John Copple, CEO of Sanborn, emphasized the broad utility of the new systems: "Our electromagnetic, magnetic, and radiometric systems are designed to produce precise geophysical maps cost-effectively, serving essential sectors such as mineral exploration, water management, transportation, energy, and construction."

Copple also emphasized Sanborn Geophysics' unique position in the marketplace. "With our acquisition last January, we have a team with decades of expertise in designing and building the geophysics sensors and systems we use.

Through Sanborn Geophysics we offer to our customers both the equipment and the end-to-end services needed for data capture, processing, and analysis.”

Copple further highlighted the advantages of Sanborn’s integrated data approach: “Geophysical data pairs well with our existing imagery, lidar, and multi-spectral data collections. With the addition of our new fixed wing airborne geophysical survey, Sanborn is leading the way in combining subsurface and surface data models to generate new insights for our clients.”



SAM, <https://www.sam.biz/>, serving utilities, transportation, and infrastructure-focused clients, today announced its acquisition of Construction Survey Technologies, Inc (CSTi), a Geospatial services and Facilities/Asset Management company based in Las Cruces, New Mexico. This acquisition strengthens SAM as a leader in Managed Geospatial Services™ and infrastructure mapping in the Southwest.

For over twenty years, CSTi has offered a wide range of services utilizing cutting-edge technology and efficient workflows to help clients minimize risk and maximize their return on investment while achieving the safest, most successful outcome.

“As SAM broadens its presence and deepens its expertise in geomatics, data visualization, and subsurface mapping services, integrating CSTi’s experience will strengthen SAM’s credibility as a trusted partner for clients seeking comprehensive Managed Geospatial Services™. We are thrilled to expand our SAM family,” said Sam Shakir, CEO of SAM.

“CSTi has positioned itself as the premier Geospatial and Asset Management Company in the Southwest, known for its innovative approach. By joining SAM, we are enhancing cutting-edge technology platforms and expanding our resources. This partnership will greatly enhance our opera-

tional capabilities, allowing us to better serve both current and new clients with advanced solutions while strategically mitigating risks and improving client relations and customer support said John Gallegos, CEO of CSTi.

Upon acquiring CSTi, SAM reaffirms its dedication to strategic growth to enhance its reputation of creating a holistic Managed Geospatial Service™ for the complete life cycle of utilities and transportation infrastructure. Entrepreneurs interested in exploring SAM’s M&A strategy are encouraged to explore our website’s “Mergers & Acquisitions” section for further details.



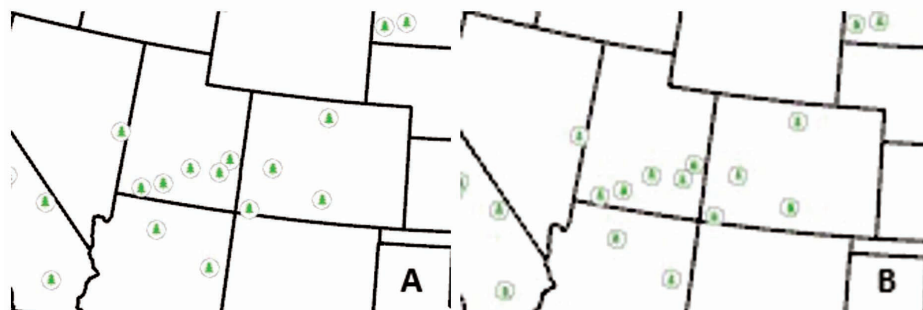
Woolpert, <https://woolpert.com/>, was selected for a five-year, \$49 million shared capacity indefinite delivery contract to provide surveying and mapping services to the U.S. Army Corps of Engineers Mobile District.

Services to be performed under this contract include airborne topographic and bathymetric lidar collection and processing; photogrammetry; topographic, boundary, hydrographic, and utility surveying; and GIS development and production and will support the district’s work for various national security, infrastructure, and emergency response planning projects. This is Woolpert’s third surveying and mapping contract for the district.

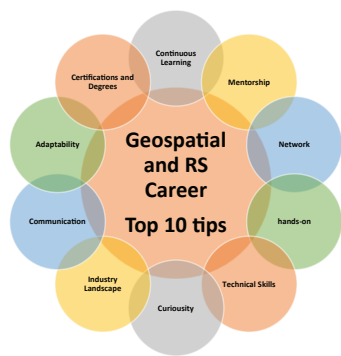
“This contract will help the Mobile District continue to successfully serve clients including the Joint Airborne Lidar Bathymetry Technical Center of Expertise, U.S. Air Force, and Department of Homeland Security,” Woolpert Vice President and National Security Program Director Darius Hensley said. “We have supported the Mobile District for nearly 20 years, and we are honored that the USACE continues to put its trust in Woolpert and our team to help successfully complete its missions.”

CALENDAR

- 7-10 October, **GIS-Pro 2024**, Portland, Maine; <https://urisa.org/page/GIS-Pro2024>.
- 8-10 October, **2024 Kentucky GIS Conference**, Louisville, Kentucky; <https://kamp.wildapricot.org/2024-Conference>.
- 8-10 October, **Kentucky GIS Conference**, Louisville, Kentucky; <https://kamp.wildapricot.org/>
- 21-25 October, **ASPRS International Technical Symposium**, virtual; <https://my.asprs.org/2024symposium>.
- 18-22 November, **URISA GIS Leadership Academy**, Fort Worth, Texas; https://urisa.org/page/URISA_AdvancedGLA.
- 2-6 December, **URISA GIS Leadership Academy**, virtual; https://urisa.org/page/URISA_AdvancedGLA.
- 10-12 February 2025, **Geo-Week**, Denver, Colorado; www.geo-week.com/



593 **GIS Tips & Tricks — When Paper Maps Just Aren't Enough**
 By Delaney Resweber and Al Karlin



595 **SectorInsight.edu — Start Strong: Top 10 Tips for a Thriving Geospatial and Remote Sensing Career**
 By Hamdy Elsayed

601 Attention Heat Map-Based Black-Box Local Adversarial Attack for Synthetic Aperture Radar Target Recognition

Xuanshen Wan, Wei Liu, Chaoyang Niu, and Wanjie Lu

Synthetic aperture radar (SAR) automatic target recognition (ATR) models based on deep neural networks (DNNs) are susceptible to adversarial attacks. In this study, we proposed an SAR black-box local adversarial attack algorithm named attention heat map-based black-box local adversarial attack (AH-BLAA).

611 Exploring the Potential of the Hyperspectral Remote Sensing Data China Orbita Zhuhai-1 in Land Cover Classification

Caixia Li, Xiaoyan Xiong, Lin Wang, Yunfan Li, Jiaqi Wang, and Xiaoli Zhang

Responding to the shortcomings of China's civil remote sensing data in land cover classification, such as the difficulty of data acquisition and the low utilization rate, we used Landsat-8, China Orbita Zhuhai-1 hyperspectral remote sensing (OHS) data, and Landsat-8 + OHS data combined with band (red, green, and blue) and vegetation index features to classify land cover using maximum likelihood (ML), Mahalanobis distance (MD), and support vector machine (SVM).

621 Teacher-Student Prototype Enhancement Network for a Few-Shot Remote Sensing Scene Classification

Ye Zhu, Shanying Yang, and Yang Yu

Few-shot remote sensing scene classification identifies new classes from limited labeled samples where the great challenges are intraclass diversity, interclass similarity, and limited supervision. To alleviate these problems, a teacher-student prototype enhancement network is proposed for a few-shot remote sensing scene classification. Instead of introducing an attentional mechanism in mainstream studies, a prototype enhancement module is recommended to adaptively select high-confidence query samples, which can enhance the support prototype representations to emphasize intraclass and interclass relationships.

631 Bank Line Extraction by Integration of Orthoimages and Lidar Digital Elevation Model Using Principal Component Analysis and Alpha Matting

Sagar S. Deshpande

Riverbank lines change over time, causing loss of land and property. Accurate mapping of riverbank lines is essential for restoration and preservation. This article presents a method to map riverbank lines by combining georeferenced orthoimages and lidar digital elevation model (DEM).

See the Cover Description on Page 592

COLUMNS

- 593** GIS Tips & Tricks — When Paper Maps Just Aren't Enough
- 595** SectorInsight.edu — Start Strong: Top 10 Tips for a Thriving Geospatial and Remote Sensing Career
- 597** Book Review — GIS TUTORIAL for ArcGIS Pro 3.1

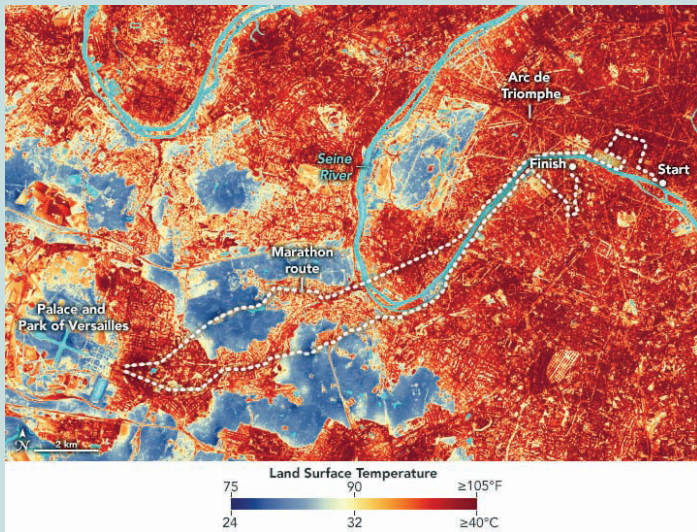
ANNOUNCEMENTS

- 599** GISCI Adds ASPRS to Board of Directors, Expanding Influence and Collaboration in Geospatial Industry
- 600** New ASPRS Members
Join us in welcoming our newest members to ASPRS

DEPARTMENTS

- 589** Industry News
- 590** Calendar
- 599** Headquarters News
- 600** Ad Index
- 610** Who's Who in ASPRS
- 619** In-Press *PE&RS* Articles
- 639** ASPRS Sustaining Members

COVER DESCRIPTION



Since Paris hosted the Olympic Games a century ago, temperatures in the city have increased by 3.1 degrees Celsius (5.5 degrees Fahrenheit). Hot days with highs above 30°C (86°F) are now nearly three times more frequent than in 1924.

The map above offers a baseline perspective on how the thermal environment along the marathon route varies on a typical summer day. It shows land surface temperatures (LSTs) observed by the VIIRS (Visible Infrared Imaging Radiometer Suite) on the NOAA-NASA Suomi NPP satellite at 1:40 p.m. local time on August 6, 2024, a clear day when air temperatures peaked at 28°C (82°F). Scientists from NASA's Jet Propulsion Laboratory "sharpened" the thermal data using machine-learning methods and surface reflectance data from the European Space Agency's Sentinel-2 satellite. The technique enhanced the resolution of the data, improving it from 375 meters per pixel to about 20 meters per pixel.

Warmer land surface temperatures are shown in red; cooler areas appear blue. Note how parks and other green infrastructure—such as the tree-lined avenues radiating from the Arc de Triomphe—are cooler than features such as buildings, roads, and parking lots. Urban spaces like these are typically constructed from materials that have a high heat capacity and absorb and re-emit the Sun's heat more than living landscapes such as trees, grass, and gardens.

The effect, known as an urban heat island, can be particularly intense in Paris, partly because the city has less tree cover than many other European cities and an abundance of zinc roofing that is particularly prone to heating up.

Note that the map shows land surface temperatures, not air temperatures. Heat islands are visible in both land surface temperatures and air temperature data, though disparities tend to be more pronounced in land surface temperatures. When the image was acquired on August 6, land surface temperatures varied from highs of 43°C (110°F) near the starting line to lows of 25°C (77°F) in thickly forested areas.

The limited tree cover in the center of Paris is visible in the other image (bottom cover), which was acquired by the OLI-2 (Operational Land Imager-2) on Landsat 9. The zinc roofing, which appears gray, can soar to temperatures of 90°C (194°F) on hot summer days.

One analysis of satellite data conducted by the European Environment Agency found that green infrastructure—urban forests and parks—cover just 26 percent of Paris, well below the 41 percent average for other European capitals. Such disparities can add up. In a recent analysis of the intensity of urban heat islands for 100 European cities, Paris came out near the top.

Both images and the complete description can be viewed online by visiting the Landsat Image Gallery, <https://landsat.visibleearth.nasa.gov/>, image id 153178.

NASA Earth Observatory images by Wanmei Liang and Michala Garrison, using VIIRS Land Surface Temperature data, marathon route from Github, and Landsat data from the U.S. Geological Survey. Story by Adam Voiland.



PHOTOGRAMMETRIC ENGINEERING & REMOTE SENSING

JOURNAL STAFF

Publisher ASPRS

Editor-In-Chief Alper Yilmaz

Director of Publications Rae Kelley

Electronic Publications Manager/Graphic Artist

Matthew Austin

Photogrammetric Engineering & Remote Sensing is the official journal of the American Society for Photogrammetry and Remote Sensing. It is devoted to the exchange of ideas and information about the applications of photogrammetry, remote sensing, and geographic information systems. The technical activities of the Society are conducted through the following Technical Divisions: Geographic Information Systems, Photogrammetric Applications, Lidar, Primary Data Acquisition, Professional Practice, Remote Sensing Applications, and Unmanned Autonomous Systems. Additional information on the functioning of the Technical Divisions and the Society can be found in the Yearbook issue of *PE&RS*.

All written correspondence should be directed to the American Society for Photogrammetry and Remote Sensing, PO Box 14713, Baton Rouge, LA 70898, including general inquiries, memberships, subscriptions, business and editorial matters, changes in address, manuscripts for publication, advertising, back issues, and publications. The telephone number of the Society Headquarters is 225-408-4747; the fax number is 225-408-4422; web address is www.asprs.org.

PE&RS. *PE&RS* (ISSN0099-1112) is published monthly by the American Society for Photogrammetry and Remote Sensing, 8550 United Plaza Blvd, Suite 1001, Baton Rouge, Louisiana 70809. Periodicals postage paid at Bethesda, Maryland and at additional mailing offices.

SUBSCRIPTION. *PE&RS* is available as an e-Subscription (single-site and multi-site licenses) and an e-Subscription with print add-on (single-site license only). *PE&RS* subscriptions are on a calendar-year, beginning in January and ending in December.

The rate for a single-site e-Subscription for the USA/Non-USA is \$1040 USD, for Canadian* is \$1092 USD.

The rate for a multi-site e-Subscription for the USA/Non-USA is \$1040 USD plus \$250 USD for each additional license, for Canadian* is \$1092 USD plus \$263 for each additional license.

The rate for e-Subscription with print add-on for the USA is \$1546 USD, for Canadian* is \$1637 USD, and for Non-USA is \$1596 USD.

*Note: Subscription prices for Canada includes 5% of the total amount for Canada's Goods and Services Tax (GST #135123065). **PLEASE NOTE: All Subscription Agencies receive a 20.00 USD discount.**

POSTMASTER. Send address changes to *PE&RS*, ASPRS, PO Box 14713, Baton Rouge, LA 70898. CDN CPM #40020812.

MEMBERSHIP. Membership is open to any person actively engaged in the practice of photogrammetry, photointerpretation, remote sensing and geographic information systems; or who by means of education or profession is interested in the application or development of these arts and sciences. Membership is for one year, with renewal based on the anniversary date of the month joined. Membership Dues include a 12-month electronic subscription to *PE&RS*. Annual Individual Membership dues are \$175.00 USD and Student Membership dues are \$50.00 USD. A tax of 5% for Canada's Goods and Service Tax (GST #135123065) is applied to all members residing in Canada.

COPYRIGHT 2024. Copyright by the American Society for Photogrammetry and Remote Sensing. Reproduction of this issue or any part thereof (except short quotations for use in preparing technical and scientific papers) may be made only after obtaining the specific approval from ASPRS. The Society is not responsible for any statements made or opinions expressed in technical papers, advertisements, or other portions of this publication. Printed in the United States of America.

PERMISSION TO PHOTOCOPY. The copyright owner's consent that copies of the article may be made for personal or internal use or for the personal or internal use of specific clients. This consent is given on the condition, however, that the copier pay the stated per copy fee through the Copyright Clearance Center, Inc., 222 Rosewood Drive, Danvers, Massachusetts 01923, for copying beyond that permitted by Sections 107 or 108 of the U.S. Copyright Law. This consent does not extend to other kinds of copying, such as copying for general distribution, for advertising or promotional purposes, for creating new collective works, or for resale.

When Paper Maps Just Aren't Enough

Among the most practical exercises in most GIS classes, including mine, is incorporating a series of historical and contemporary maps and images into a project and mapping the changes over a time period, i.e. change detection. Sometimes, you get lucky and all of the maps/images include “world files” or Geotiff tags that enable your GIS to spatially index the maps/images and everything fits. However, most of the time, you don't get so lucky and the maps/images are not “georeferenced”. The good news is that most GIS software packages provide for some level of assigning real-world coordinates, in a projected coordinate reference system (CRS), to those “raw” maps/images. The process of assigning those coordinates and indexing the raw images to a CRS is called “georeferencing”.

Georeferencing is a great way to incorporate digitally scanned maps and other images into a GIS dataset. From scans of historical parchment maps from the 1600s, to Computer Aided Drafting (CAD) city-drafted utility maps created in the 1980s, to scanned modern paper maps for which we do not always have the GIS data layers, there are many instances where you might want to georeference either the electronic computer aided design (CAD files; .DXF/.DWG) InterGraph Design files (.DNG) or scans and images; Joint Photographic Experts Group; Tagged Image File, International Management Group, or Portable Network Graphic (.JPG, .TIF, .IMG, .PNG, etc.), as well as those paper maps, so they can be used as layers in your GIS.

This month, I am collaborating with Delaney Resweber to provide some tips and tricks that she's learned over the years to make georeferencing easier!

TIP #1 — START WITH A HIGH-RESOLUTION IMAGE; THE HIGHER THE BETTER!

Ideally, the image you are georeferencing is a high-resolution .TIF, .JPG, etc. file, 300 dots per inch (DPI) or greater. Crisper details on the image allow you to more accurately choose control points (see TIP #3) which results in better aligning the map geospatially, which, in turn, results in a better product. Starting with a high resolution image makes any of the maps you create easier to read and more professional looking, and if you ever decide to take the additional steps of heads-up digitizing the map into one or more vector layers, it will make that process a lot smoother. As an example, in Figure 1, one map was scanned at 50 DPI (A) and the other 300 DPI (B). The difference in resolution is easily observable.



Figure 1. A portion of a map showing National Parks in the western U.S. Map A was scanned at 300 DPI while Map B was scanned at 50 DPI.

Often, we aren't lucky, and we start with a low-resolution image, as in historical images where you take whatever you can get, or you are stuck with a scan of a scan in Page Description Format form; the worst of all possible worlds. Luckily, there are ways to work around this, including using Adobe Illustrator, Adobe Photoshop or similar programs to increase the image resolution with Artificial Intelligence (AI) image enhancing technologies (beyond the scope of this article).

Photogrammetric Engineering & Remote Sensing
Vol. 90, No. 10, October 2024, pp. 593-594, 600.
0099-1112/22/593-594, 600

© 2024 American Society for Photogrammetry
and Remote Sensing
doi: 10.14358/PERS.90.10.593

TIP #2 — DON'T BE AFRAID TO CROP THE IMAGE

Sometimes the image you are georeferencing was not captured to the spatial extent of your project. A typical example may be a Department of Transportation (DOT) or Natural Resources Conservation Service (NRCS) 1:24,000 scanned photograph showing more area than you need. This may make it very difficult to place control points (TIP #3) that allow the image to line up with its real-world locations.

To resolve this, you can crop the image into multiple parts in Adobe Photoshop, Microsoft Paint, or similar programs and align those parts individually if needed. This allows you to place control points specific to those regions and not worry about the rest of the image being skewed as a result.

TIP #3 — PLACE AT LEAST FIVE CONTROL POINTS

The process that GIS software (and photogrammetric packages) use to georeference images requires the user to identify a point (pixel) on the image, in image coordinates, and its real-world cognate coordinates in the desired CRS. The workflow described below is for general reference as more detailed instructions are available at: <https://pro.arcgis.com/en/pro-app/latest/help/data/imagery/georeferencing-a-raster-to-a-referenced-layer.htm> and/or the videos available on YouTube (<https://www.youtube.com/watch?v=3r7ELaxRdDs>).

IN ARCGIS PRO

Step 1 — The workflow starts with adding the non-georeferenced image, scan or electronic file to a map frame containing a source raster or vector that is properly georeferenced and is referenced to a real CRS.

Step 2 — ArcGIS Pro 3.3 will detect a non-georeferenced image and add a “Georeference Tab” (Figure 2) to the ribbon. In previous versions, you may need to use the Imagery Tab to activate the Georeference Tab.

Step 3 — In ArcGIS Pro, use the “Fit to Display” function on the Georeferencing toolbar to move the non-georeferenced image into the general map space. The image will NOT be scaled or georeferenced, but it will be visible on the map.

Step 4 — Use the “Add Control Points” tool to draw links between the non-georeferenced image and the CRS in your

map frame. This tool allows the user to draw a line (called a link) starting at the non-georeferenced layer and ending on the georeferenced layer at the cognate location, the “control point”. I tell my students that the links ALWAYS go from the picture to the ground!

Step 5 — These “control points” and links are then used to mathematically transform all of the pixels in the non-georeferenced image (scan or electronic file) to their real-world coordinates. Most GIS software packages offer multiple transformations (beyond the scope of this Tips & Tricks article.)

Try to place at least four control points around the four corners of image with the final, fifth point placed somewhere near the center of the image. This allows the image to more appropriately adjust to the correct location rather than be skewed one way or the other with the transformation applied. If you place all your control points on the northeastern portion of the image, then it's not going to be aligned the right way in the rest of the image and could be badly misaligned.

TIP #4 — FIND LANDMARKS FOR CONTROL POINTS

When placing control points, be conscientious of the features your image has mapped versus what the basemap or the imagery layer you're using to georeference your image displays. Avoid placing your control points on arbitrary features that may vary map to map, such as contour lines or wetland boundaries. Try using road intersections, river intersections or building corners (but remember that building corners may display parallax displacement.)

Sometimes you have to get creative. For example, with one of my projects I was georeferencing underground subway plans - so I lined up the street entrances of the subway with the entrance level plans, connecting the entryways. Then, I connected the other levels to this entrance level plan without using the imagery.

TIP #5 — EXPERIMENT WITH NEW TOOLS

The GIS world is always expanding and innovating with new solutions and programs. Keep up to date on what other professionals are doing and try experimenting outside of the tried and true to elevate what you can do with your georeferenced imagery.

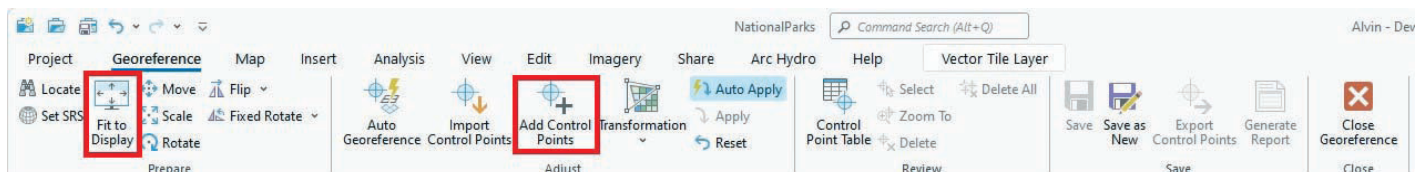


Figure 2. The Georeference Tab in ArcGIS Pro 3.3.

continued on page 600



Hamdy Elsayed, Ph.D., Head of Innovation, *Teledyne Geospatial*



Start Strong: Top 10 Tips for a Thriving Geospatial and Remote Sensing Career

Navigating a successful career in the geospatial engineering, photogrammetry, and remote sensing industry requires a blend of technical expertise, continuous learning, and strategic networking. Here are ten essential tips to help students and early career professionals thrive in this dynamic field:

Embrace Continuous Learning

The geospatial and remote sensing industry is constantly evolving with new technologies and methodologies. Staying updated with the latest advancements is crucial. Enroll in online courses, attend workshops and conferences, and read industry publications. Platforms like Coursera and edX offer various courses in remote sensing and photogrammetry. Subscribing to journals like ASPRS PE&RS or joining organizations such as the Canadian Remote Sensing Society (CRSS) can keep you informed about the latest research and trends. Industry publications like Inside GNSS, Inside UAV, and LiDAR Magazine are also great sources for the state-of-the-art technologies in our field.

To ensure you're always on the cutting edge, consider setting aside regular time each week to study new developments. This could involve reading the latest research papers, experimenting with new software tools, or participating in webinars. Continuous learning not only keeps your skills relevant but also demonstrates to employers your commitment to professional growth.

Seek Mentorship

Having a mentor can provide invaluable guidance and support. Look for experienced professionals who can offer advice, share their experiences, and help you develop your skills. Platforms like LinkedIn can be used to connect with potential mentors. Professional organizations, such as ASPRS, often have mentorship programs designed to pair early career professionals with experienced mentors. Mentors can provide insights into different career paths; help you make informed decisions about your professional development.

When seeking a mentor, consider what specific skills or knowledge you want to develop and look for someone whose expertise aligns with those areas. Regularly meet with your mentor to discuss your progress and challenges. Mentorship is a two-way street; be sure to bring value to your mentor by showing appreciation and applying their advice effectively.



Additionally, the ASPRS ECPC Mentorship Podcast is an excellent resource where experienced professionals share their insights and advice.

Build a Strong Network

Networking is essential for career advancement. Attend industry events, join professional organizations like ASPRS, ISPRS, and CRSS, and connect with peers and experts. Participating in conferences such as the ISPRS Congress or the ASPRS Annual Conference can help you meet key industry players and stay updated on the latest developments.

Effective networking involves more than just meeting people; it's about building lasting relationships. Follow up with new contacts after events, engage with their content on social media, and offer your assistance when possible. Networking can lead to job opportunities, collaborations, and valuable industry insights.

Photogrammetric Engineering & Remote Sensing
Vol. 90, No. 10, October 2024, pp. 595-596, 600.
0099-1112/22/595-596, 600

© 2024 American Society for Photogrammetry
and Remote Sensing
doi: 10.14358/PERS.90.10.595

Gain Practical Experience

Hands-on experience is critical for bridging the gap between academic knowledge and industry requirements. Seek internships, part-time jobs, or volunteer opportunities that allow you to apply your skills in real-world settings. Websites like Indeed, Glassdoor, and company career pages are great resources for finding internships and positions in the geomatics and remote sensing field. Many companies and organizations offer internships that allow you to work on real-world projects and gain practical experience.

During internships, be proactive in taking on challenging tasks and learning as much as possible. Ask questions, seek feedback, and strive to understand how your work contributes to larger projects. Practical experience not only enhances your resume but also gives you a clearer understanding of your career interests and goals.

Develop Technical Skills

Proficiency in remote sensing technologies is a must. Familiarize yourself with tools and software used in photogrammetry, lidar, and data processing. Online tutorials, courses, and certifications from providers like ASPRS can help enhance your technical skills. For photogrammetry, learn to use software like Pix4D and Agisoft Metashape. For lidar processing, gain proficiency in software such as Terrasolid and LAStools. For radar remote sensing, understand the principles and learn to process radar data using software like ESA's Sentinel-1 Toolbox.

Beyond software skills, understanding the theoretical principles behind these technologies is equally important. Study the physics of remote sensing, data acquisition methods, and processing algorithms. This deep knowledge will enable you to troubleshoot problems effectively and innovate within your field.

Stay Curious

The geomatics field thrives on innovation. Explore new ideas and approaches, whether it's developing a new application for lidar data or finding novel ways to analyze remote sensing information. Engage with communities on platforms like GitHub for open-source projects and Kaggle for data science competitions. Stay curious by joining competitions and exploring the potential of emerging technologies such as machine learning and artificial intelligence in remote sensing applications.

Innovation often comes from looking at problems from different perspectives. Collaborate with professionals from other disciplines, attend interdisciplinary conferences, and read broadly outside your immediate field. By combining insights from various sources, you can develop unique solutions and advance the state of the art in geospatial sciences.

Understand the Industry Landscape

A good grasp of the industry landscape is essential for identifying opportunities and making informed career decisions. Stay informed about key players, market trends, and emerging technologies in the geospatial and remote sensing sector. Reading industry reports, following key companies on social media, and subscribing to industry newsletters can provide valuable insights. Track developments at major companies like Teledyne, Hexagon, and Trimble. Subscribe to newsletters and websites such as Geospatial World or GIM International for updates on the latest industry news, technological advancements, and market trends.

Understanding the competitive landscape can help you identify gaps in the market where your skills and interests align. It can also guide you in choosing employers and projects that match your career aspirations.

Communicate Effectively

Strong communication skills are vital for collaborating with colleagues, presenting your work, and advocating for your ideas. Practice clear and concise communication, whether through writing reports, giving presentations, or engaging in discussions. Additionally, joining a local Toastmasters club can provide practical experience and feedback.

Effective communication involves tailoring your message to your audience. Whether you're explaining technical details to a non-expert or presenting a business case to stakeholders, clarity and relevance are key. Practice active listening, ask for feedback, and continuously refine your communication style to become more persuasive and impactful.

Adapt to Change

The geospatial and remote sensing industry is dynamic, with continually evolving technologies and methodologies. Being adaptable and open to change is crucial for long-term success. Stay flexible and willing to learn new skills as the industry evolves. Embrace new technologies and methodologies as they emerge and be prepared to pivot your career focus as needed.

Adaptability also means being resilient in the face of setbacks. The ability to learn from failures, adjust your approach, and persevere is critical for sustaining a successful career. Cultivate a growth mindset that views challenges as opportunities for learning and development.

Pursue Certifications and Advanced Degrees

Pursuing additional certifications or advanced degrees can enhance your qualifications and open new career opportunities. Advanced credentials can demonstrate your expertise and commitment to the field. Obtain Certified Photogrammetrist or Certified Mapping Scientist credentials from ASPRS. Enroll in advanced degree programs that focus on geomatics,

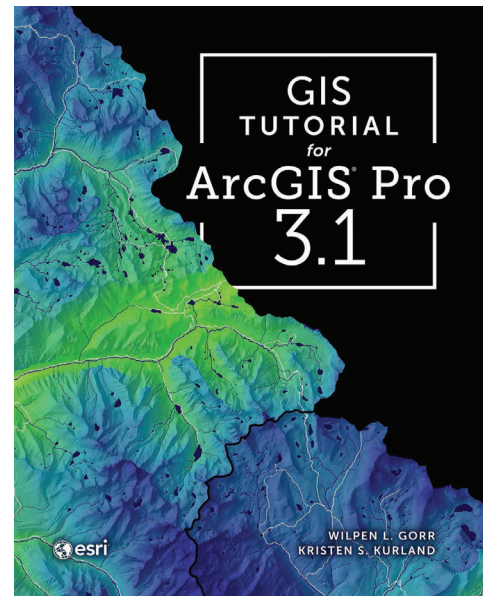
continued on page 600

The fifth edition of the *GIS Tutorial for ArcGIS Pro 3.1* by Wilpen L. Gorr and Kristen S. Kurland is valuable for anyone looking to master Esri's flagship GIS software. Whether you are a student, educator, or professional, this book offers a step-by-step approach to learning the latest tools in ArcGIS Pro 3.1 through tutorials and assignments. With 11 chapters, the book is divided into three parts. The first part comprises of three chapters focusing on using, making, and sharing maps; the second part focuses on map design and includes five chapters; and the third part focuses on applying advanced GIS technologies and has three chapters. The book builds user's skills gradually, starting with an overview of ArcGIS Pro and culminating in advanced techniques for geoprocessing, network analysis, raster analysis, and 3D data manipulation.

Chapter 1 summarizes ArcGIS Pro with tutorials on ArcGIS Pro project setup, navigation, and working with attribute data. Chapter 2 focuses on symbolizing and labeling features, filtering data, creating various maps, and exploring cartographic principles. Chapter 3 focuses on creating user-friendly maps with layouts, charts, and interactive elements and sharing the work through ArcGIS Online, ArcGIS StoryMaps, and Dashboards. Chapter 4 focuses on data management, explaining how to create geodatabases, import and modify data, and perform attribute and spatial

***Whether you are a student,
educator, or professional,
this book offers a step-by-step
approach to learning the
latest tools in ArcGIS Pro 3.1***

queries. Chapter 5 covers topics on map projection systems, vector data formats, and geospatial data acquisition. Chapter 6 applies geoprocessing tools for data analysis, transformation, and overlay to derive valuable insights. In Chapter 7, users learn how to create, modify, update, and digitize vector map features within ArcGIS Pro. Chapter 8 covers the topics of the geocoding process, with tutorials on geocoding using zip codes and street addresses. Chapter 9 covers a range of spatial analysis techniques, including proximity analysis, overlay analysis, and network analysis. Chapter 10 introduces raster datasets, covering topics on raster processing and the application of ArcGIS Pro model builder for developing raster-based models. Chapter 11 covers topics on 3D GIS data visualization processing and feature creation.



GIS TUTORIAL for ArcGIS Pro 3.1

Wilpen L. Gorr, Kristen S. Kurland. Esri Press, Redlands, CA. 2023. xiv and 298 pp., diagrams, maps, photos, images. Paperback. List price \$119.99. ISBN 978-1-58948-739-0.

Reviewed by Abishek Poudel, PhD Candidate, Department of Sustainable Resources Management, SUNY College of Environmental Science and Forestry, Syracuse, NY.

The book is accompanied by online resources, including downloadable data and teaching slides, which can help instructors use the book in a classroom setting. Each chapter includes current, real-world data in the tutorials and assignments that add relevance and the practical applications of GIS concepts. This book is specifically tailored to ArcGIS Pro 3.1. However, most concepts and techniques also apply to newer software versions. The authors excel at simplifying intricate subjects, ensuring the book is a user-friendly resource for learners at any level.

The “GIS Tutorial for ArcGIS Pro 3.1” offers a comprehensive guide to mastering ArcGIS Pro. Its structured approach, simple explanations, and practical tutorials make it a go-to guide for students, professionals, and GIS enthusiasts.

Photogrammetric Engineering & Remote Sensing
Vol. 90, No. 10, October 2024, pp. 597.
0099-1112/22/597

© 2024 American Society for Photogrammetry
and Remote Sensing
doi: 10.14358/PERS.90.10.597

MAP, EXTRACT & DELIVER WITH PIXELEMENT

PixElement creates production-grade photogrammetry software for geospatial, land surveying, and engineering professionals that is used throughout the world. We offer our software in cloud and desktop environments, empowering our users in the field, in the office, or wherever their work takes them. Whether mapping small subdivision-scale sUAS missions or large city-scale mapping surveys from aircraft, PixElement scales with your business needs and resource requirements. By allowing users to upload their project data, whether it be imagery data for photogrammetry mapping or combining multiple modalities like lidar, imagery and vector data for fused deliverables, PixElement is designed to meet the rigorous demands of geospatial professionals and enables them to create different geospatial data products such as point clouds, textured 3D meshes, orthomosaics, and more.



2D Orthomosaic with annotations and measurements made in PixElement

A unique feature that PixElement offers is lidar integration with imagery projects. This allows users to achieve higher levels of detail and accuracy while also correcting for modeling errors commonly experienced with lidar datasets. Bore-sight alignment and other calibration errors can cause small and large deviations between what the camera sensor on the drone captures and what the lidar sensor captures. These corrections allow for users to extract maximum quality with their models.



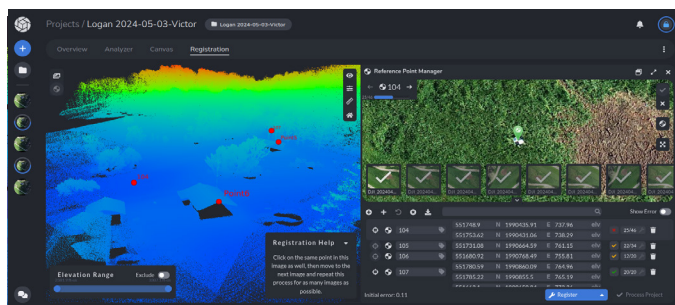
Uncorrected versus corrected lidar point cloud models

PixElement allows for the implementation of ground control points (GCPs) and manual tiepoints within the project to improve model accuracy and ensure cohesive, well-aligned models. The automatic reference point extraction feature allows for quick identification of ground control points so users can quickly and accurately process their project. Furthermore, PixElement's intuitive interface and powerful

processing capabilities optimize the workflow, enabling users to easily import, process, and visualize their combined lidar + imagery or solely imagery datasets. Automated tools within the platform facilitate the alignment and calibration of these datasets, ensuring accuracy and consistency across the entire project.



Mesh of lidar collected data downtown Miami, Florida



View of Reference Point Manager lidar registration with elevation

PixElement serves many industries, especially those in the mining, land surveying and construction sectors with project sizes varying from small construction projects to large quarries with thousands of images. Users are able to annotate their projects with tools such as adding points, polylines and polygons, requesting linework and are further able to generate grids, bare earth TINs, and contours, all while managing their layers in the drawing manager.

Deliverables renderable by PixElement include: point cloud, digital elevation model, textured 3D mesh, and orthomosaic, all available in a variety of exportable formats (obj, las, ffw, jpg, jgw) to ensure compatibility with industry-standard software and GIS platforms.

Visit www.PixElement.com to learn more or try out a free 14-day trial.



JOURNAL STAFF

Editor-In-Chief

Alper Yilmaz, Ph.D., PERSEditor@asprs.org

Associate Editors — Photogrammetry

Rongjun Qin, Ph.D., qin.324@osu.edu

Petra Helmholtz, Ph.D., Petra.Helmholtz@curtin.edu.au

Bo Wu, Ph.D., bo.wu@polyu.edu.hk

Filiz Sunar, Ph.D., fsunar@itu.edu.tr

Dorota Iwaszczuk, Ph.D., dorota.iwaszczuk@tum.de

Jan Dirk Wegner, Ph.D., jan.wegner@geod.baug.ethz.ch

Associate Editors — Remote Sensing

Valérie Gouet-Brunet, Ph.D., valerie.gouet@ign.fr

Prasad Thenkabail, Ph.D., pthenkabail@usgs.gov

Desheng Liu, Ph.D., liu.738@osu.edu

Qunming Wang, Ph.D., wqm11111@126.com

Hongyan Zhang, Ph.D., zhanghongyan@whu.edu.cn

Zhenfeng Shao, Ph.D., shaozhenfeng@whu.edu.cn

Dongdong Wang, Ph.D., ddwang@umd.edu

Sidike Paheding, Ph.D., spahedin@mtu.edu

Ribana Roscher, Ph.D., ribana.roscher@uni-bonn.de

Ruisheng Wang, Ph.D., ruiswang@ucalgary.ca

John Rogan, Ph.D., jrogan@clarku.edu

Ravi Shankar Dwivedi, Ph.D., rsdwivedi51@gmail.com

Contributing Editors

Highlight Editor

Jie Shan, Ph.D., jshan@ecn.purdue.edu

Feature Articles

Michael Joos, CP, GISP, featureeditor@asprs.org

Grids & Datums Column

Clifford J. Mugnier, C.P., C.M.S., cjmce@lsu.edu

Book Reviews

Sagar Deshpande, Ph.D., bookreview@asprs.org

Mapping Matters Column

Qassim Abdullah, Ph.D., Mapping_Matters@asprs.org

GIS Tips & Tricks

Alvan Karlin, Ph.D., CMS-L, GISP akarlin@Dewberry.com

SectorInsight

Youssef Kaddoura, Ph.D., kaddoura@ufl.edu

Bob Ryerson, Ph.D., FASPRS, bryerson@kingeomatics.com

Hamdy Elsayed, Hamdy.Elsayed@teledyne.com

ASPRS Staff

Assistant Director — Publications

Rae Kelley, rkelly@asprs.org

Electronic Publications Manager/Graphic Artist

Matthew Austin, maustin@asprs.org

Advertising Sales Representative

Bill Spilman, bill@innovativemediasolutions.com

GISCI ADDS ASPRS TO BOARD OF DIRECTORS, EXPANDING INFLUENCE AND COLLABORATION IN GEOSPATIAL INDUSTRY

The GIS Certification Institute (GISCI) is pleased to announce its new partnership with the American Society for Photogrammetry and Remote Sensing (ASPRS), with ASPRS joining GISCI's Board of Directors. This strategic move represents a significant milestone in the ongoing efforts to advance geospatial science, promote best practices, and support professional development within the industry.

"We are thrilled to have ASPRS join our board," said Jochen Albrecht, Chair of the GISCI Board. "ASPRS's deep knowledge and experience in remote sensing and photogrammetry will be instrumental in shaping the future of geospatial certification and professional development."

As a new board member, ASPRS will contribute its extensive expertise in remote sensing and photogrammetry to GISCI's initiatives. This partnership will help bridge gaps between different sectors of the geospatial field, offering a more comprehensive perspective on industry challenges and opportunities.

"The inclusion of ASPRS on the GISCI Board of Directors marks an exciting new chapter for both organizations," said Bandana Kar, President of ASPRS. "Our shared mission to elevate the geospatial profession and support its practitioners align perfectly with GISCI's goals. We look forward to working closely with GISCI to drive forward initiatives that will benefit the entire geospatial community."

The collaboration is expected to yield a range of benefits, including enhanced certification programs, joint educational initiatives, and a unified approach to addressing key issues facing the geospatial industry. Both organizations are committed to leveraging their combined strengths to advance the field and support professionals across various geospatial disciplines.

PE&RS RANKS IN THE TOP 10 ON INGENTACONNECT

PE&RS continues to rank in the top 10 in downloads on IngentaConnect

Ranked 9th in March and May, 8th in April, 11th in June, and 10th in July.

GIS Tips & Tricks, continued from page 594

Recently, Bunting Labs created a [QGIS plug-in](#) that automates the vectorization process of taking georeferenced imagery and digitizing it into vector layers. ESRI has developed unique ways to incorporate georeferenced maps using their [Story Maps](#) application, allowing a larger audience to interact with maps in an easy to navigate web interface. In addition, it is a great tool to help tell stories and narratives supported by text, audio and video medias.

Send your questions, comments, and tips to GISTT@ASPRS.org.

Delaney Resweber is a GIS Analyst with Dewberry's Geospatial and Technology Services group in Fairfax, VA. Her specialties are creating GIS application solutions and cultural resources.

Al Karlin, Ph.D., CMS-L, GISP is with Dewberry's Geospatial and Technology Services group in Tampa, FL. As a senior geospatial scientist, Al works with all aspects of lidar, remote sensing, photogrammetry, and GIS-related projects.

Ad Index

PixElement | pixelement.com/ | 598

SectorInsight.edu, continued from page 596

photogrammetry, or remote sensing. Certifications and advanced degrees not only validate your skills but also expand your professional network through interactions with peers and instructors. They can lead to higher-paying jobs, leadership roles, and opportunities to contribute to cutting-edge research and development projects.

Author

Hamdy Elsayed, PhD, the head of Innovation at Teledyne Geospatial, is an expert in the field of geospatial and remote sensing, known for his significant contributions to both academia and industry. With a robust academic background and extensive professional experience, Hamdy has established himself as a leader and innovator in the geospatial community. His commitment to excellence and passion for geospatial science inspire those around him and drive his ongoing contributions to the field. Hamdy believes in the transformative power of geospatial technologies and their potential to address some of the world's most pressing challenges. He advocates for a holistic approach that integrates scientific research, technological innovation, and practical application.

NEW ASPRS MEMBERS

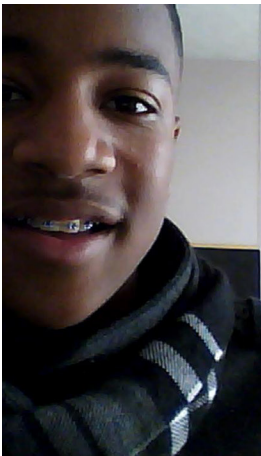
ASPRS would like to welcome the following new members!

Paul Bishop
Cole Bramel
Grace Braver
Kayde Renae Bruce
Aditya Eaturu
Justus Eckstrom
Annastasia Erdmann
Carlos E. Genatios, PhD
Darren Goodding
Chris Hunt

Hayder Hameed Jassoom
Ramesha Kumbara
Nicklaus Allen Kuntzman
James Ryan LaValle
Anil Kumar Mandal
Charles Michael Mansfield, III
Noah Morris
Joshua Noel
Nicholas Pardy
Steph Phillips

Tonya Prine
BreeLynn Robinson
George Rogers
Colin Sahs
Anna Sherrill
Raihan Sorker
Mitchell Stewart
Weilun Tay
Holly Torpey, GISP
John Wall, PhD

FOR MORE INFORMATION ON ASPRS MEMBERSHIP, VISIT [HTTP://WWW.ASPRS.ORG/JOIN-NOW](http://www.asprs.org/join-now)



**Too young to drive the car? Perhaps!
But not too young to be curious about geospatial sciences.**

The ASPRS Foundation was established to advance the understanding and use of spatial data for the betterment of humankind. The Foundation provides grants, scholarships, loans and other forms of aid to individuals or organizations pursuing knowledge of imaging and geospatial information science and technology, and their applications across the scientific, governmental, and commercial sectors.

Support the Foundation, because when he is ready so will we.

asprsfoundation.org/donate



Attention Heat Map-Based Black-Box Local Adversarial Attack for Synthetic Aperture Radar Target Recognition

Xuanshen Wan, Wei Liu, Chaoyang Niu, and Wanjie Lu

Abstract

Synthetic aperture radar (SAR) automatic target recognition (ATR) models based on deep neural networks (DNNs) are susceptible to adversarial attacks. In this study, we proposed an SAR black-box local adversarial attack algorithm named attention heat map-based black-box local adversarial attack (AH-BLAA). First, we designed an attention heat map extraction module combined with the layer-wise relevance propagation (LRP) algorithm to obtain the high concerning areas of the SAR-ATR models. Then, to generate SAR adversarial attack examples, we designed a perturbation generator module, introducing the structural dissimilarity (DSSIM) metric in the loss function to limit image distortion and the differential evolution (DE) algorithm to search for optimal perturbations. Experimental results on the MSTAR and FUSAR-Ship datasets showed that compared with existing adversarial attack algorithms, the attack success rate of the AH-BLAA algorithm increased by 0.63% to 33.59% and 1.05% to 17.65%, respectively. Moreover, the low-level perturbation ratios reached 0.23% and 0.13%, respectively.

Introduction

A primary advantage of synthetic aperture radar (SAR) is its ability to acquire target images all day under all weather conditions. Consequently, it is widely used in both military and civilian fields (Brown 1967; Moreira *et al.* 2013; Zhang *et al.* 2018). Recently, deep neural network (DNN) models have achieved remarkable results in synthetic aperture radar (SAR) automatic target recognition (ATR) systems (Chen 2016; Ding *et al.* 2016; Du *et al.* 2016; Vint *et al.* 2016; Zhang *et al.* 2017). However, SAR-ATR based on DNN models are vulnerable to adversarial attacks. The attacker can cause the DNN models to output incorrect results by adding small perturbations to the input SAR image. At the same time, perturbations in the image domain have been shown to be physically achievable. Researchers have established connections between the image domain and the physical domain (Dang *et al.* 2021; Peng *et al.* 2022; Qin and Wang 2023; Xia *et al.* 2023; Zhou *et al.* 2023; Ji *et al.* 2023; Cui *et al.* 2024). Therefore, studying perturbation generation in the image domain is the theoretical basis and the first step to realize physical attacks, which is of great significance and value. First, based on the adversarial perturbation in the image domain, we can realize adversarial attack by placing the absorbing material or strong scatterer on the target surface. Then, we can convert the perturbation in the image domain to jamming signal by combining the deception jamming technology and the parameter information of the opponent's SAR system. The defender can use adversarial examples to augment the training data to fine-tune their own SAR-ATR model to enhance its robustness.

Adversarial attacks on neural network models were first investigated in the optical imaging field. Depending on whether the attacker

knows the victim model, adversarial attack algorithms can be divided into white-box and black-box attacks. White-box attacks require knowledge of the victim model's information. Typical attack methods include the gradient (Goodfellow *et al.* 2014; Kurakin *et al.* 2018), boundary (Moosavi-Dezfooli *et al.* 2016), and saliency map-based (Papernot *et al.* 2016) attacks. Conversely, in a black-box attack scenario, an attacker finds obtaining information from the victim model difficult. Black-box attacks can be divided into probabilistic label-based (Chen *et al.* 2017; Su *et al.* 2019), decision-based (Chen *et al.* 2020), and transfer-based (Xie *et al.* 2019) attacks.

Adversarial attack examples have also appeared in the SAR-ATR field (Du *et al.* 2022; Xia *et al.* 2023). Huang *et al.* (2020) used the fast gradient sign method (FGSM) and basic iterative method (BIM) algorithms to verify the existence of adversarial attack examples in the SAR-ATR field. To limit perturbations to a target area, Meng *et al.* (2022) proposed the target region perturbation generator (TRPG) algorithm, which first used the Gabor algorithm to perform texture segmentation on the SAR image to obtain the target area mask before constructing perturbations within the target area. Peng *et al.* (2021) proposed an SAR image adversarial attack algorithm named target segmentation-based adversarial attack (TSAA), which only added perturbations to the target area and successfully attacked the mainstream DNN models.

However, there are still several problems with the aforementioned algorithms:

- (1) From an attack targeting perspective, existing local adversarial attack algorithms primarily use image segmentation algorithms to obtain target and background areas. However, the attack perturbation range against the DNN model should be limited to areas of focus on the model. Consequently, the development of perturbation algorithms that limit perturbations to regions of focus on the DNN model is needed.
- (2) From an attack concealment perspective, attack concealment is challenging and must be improved because the disturbed areas are still large.
- (3) Based on the noncooperative characteristics analysis of SAR attacks, adversarial attacks should be able to proceed even without sufficient SAR-ATR information. However, existing local SAR attack algorithms must use the gradient information of DNN models. Consequently, there is a need for local adversarial attack algorithms to operate under black-box conditions.

To solve the aforementioned problems, we proposed an SAR black-box local adversarial attack algorithm called the attention heat map-based black-box local adversarial attack (AH-BLAA) algorithm. First, we designed an attention heat map extraction module, which used the layer-wise relevance propagation (LRP) (Bach *et al.* 2015) algorithm to generate an attention heat map of the DNN models. Subsequently, the attention heat map was used to locate the perturbation range in

Xuanshen Wan, Wei Liu, Chaoyang Niu, and Wanjie Lu are with Information Engineering University.

Corresponding author: Wei Liu (greatliuliu@163.com)

Contributed by Ribana Roscher, February 23, 2024 (sent for review April 3, 2024; reviewed by Gang Hong, Liangpei Zhang).

Photogrammetric Engineering & Remote Sensing
Vol. 90, No. 9, October 2024, pp. 601–609.
0099-1112/22/601-609

© 2024 American Society for Photogrammetry
and Remote Sensing
doi: 10.14358/PERS.24-00015R2

**PEER-REVIEWED CONTENT
IS ONLY AVAILABLE TO
ASPRS MEMBERS AND SUBSCRIBERS**

**FOR MORE INFORMATION VISIT
[MY.ASPRS.ORG](https://my.asprs.org)**

**PEER-REVIEWED CONTENT
IS ONLY AVAILABLE TO
ASPRS MEMBERS AND SUBSCRIBERS**

**FOR MORE INFORMATION VISIT
[MY.ASPRS.ORG](https://my.asprs.org)**

**PEER-REVIEWED CONTENT
IS ONLY AVAILABLE TO
ASPRS MEMBERS AND SUBSCRIBERS**

**FOR MORE INFORMATION VISIT
[MY.ASPRS.ORG](https://my.asprs.org)**

**PEER-REVIEWED CONTENT
IS ONLY AVAILABLE TO
ASPRS MEMBERS AND SUBSCRIBERS**

**FOR MORE INFORMATION VISIT
[MY.ASPRS.ORG](https://my.asprs.org)**

**PEER-REVIEWED CONTENT
IS ONLY AVAILABLE TO
ASPRS MEMBERS AND SUBSCRIBERS**

**FOR MORE INFORMATION VISIT
[MY.ASPRS.ORG](https://my.asprs.org)**

**PEER-REVIEWED CONTENT
IS ONLY AVAILABLE TO
ASPRS MEMBERS AND SUBSCRIBERS**

**FOR MORE INFORMATION VISIT
[MY.ASPRS.ORG](https://my.asprs.org)**

**PEER-REVIEWED CONTENT
IS ONLY AVAILABLE TO
ASPRS MEMBERS AND SUBSCRIBERS**

**FOR MORE INFORMATION VISIT
[MY.ASPRS.ORG](https://my.asprs.org)**

**PEER-REVIEWED CONTENT
IS ONLY AVAILABLE TO
ASPRS MEMBERS AND SUBSCRIBERS**

**FOR MORE INFORMATION VISIT
[MY.ASPRS.ORG](https://my.asprs.org)**

WHO'S WHO IN ASPRS

Founded in 1934, the American Society for Photogrammetry and Remote Sensing (ASPRS) is a scientific association serving thousands of professional members around the world. Our mission is to advance knowledge and improve understanding of mapping sciences to promote the responsible applications of photogrammetry, remote sensing, geographic information systems (GIS) and supporting technologies.

BOARD OF DIRECTORS

BOARD OFFICERS

President

Bandana Kar
U. S. Department of Energy (DOE)

Vice President

Alvan Karlin, PhD, CMS-L, GISP
Dewberry

Treasurer

John McCombs
NOAA

President-Elect

Amr Abd-Elrahman
University of Florida

Past President

Lorraine B. Amenda, PLS, CP
Towill, Inc

Secretary

Harold Rempel
ESP Associates, Inc.

COUNCIL OFFICERS

ASPRS has six councils. To learn more, visit <https://www.asprs.org/Councils.html>.

Sustaining Members Council

Chair: Paul Badr
Deputy Chair: Melissa Martin

Early-Career Professionals Council

Chair: Greg Stamnes

Committee Chairs Council

Chair: David Day

Technical Division Directors Council

Chair: Hope Morgan
Deputy Chair: Tao Liu

Region Officers Council

Chair: Demetrio Zourarakis
Deputy Chair: Cody Condron

Student Advisory Council

Chair: Oscar Duran
Deputy Chair: Ali Alruzuq

TECHNICAL DIVISION OFFICERS

ASPRS has seven professional divisions. To learn more, visit <https://www.asprs.org/Divisions.html>.

Geographic Information Systems Division

Director: Jin Lee
Assistant Director: Michael Baranowski

Photogrammetric Applications Division

Director: Hank Theiss
Assistant Director: Jae Sung Kim

Remote Sensing Applications Division

Director: Tao Liu
Assistant Director: Indu Jeyachandran

Lidar Division

Director: Matt Bethel
Assistant Director: Nora May

Primary Data Acquisition Division

Director: Srinu Dharmapuri
Assistant Director: Ravi Soneja

Unmanned Autonomous Systems (UAS)

Director: Bahram Salehi
Assistant Director: Rebecca Capps

Professional Practice Division

Director: Hope Morgan
Assistant Director: Christian Stallings

REGION PRESIDENTS

ASPRS has 13 regions to serve the United States. To learn more, visit <https://www.asprs.org/regions.html>.

Alaska Region

Dave Parret

Gulf South

Cody Condron

Pacific Southwest Region

Omar Mora

Cascadia Region

Jimmy Schulz

Heartland Region

Whit Lynn

Potomac Region

Jason Brown

Eastern Great Lakes Region

Craig Fry

Mid-South Region

David Hughes

Rocky Mountain Region

Trent Casi

Florida Region

Matt LaLuzerne

North Atlantic Region

Kurt Lutz

Western Great Lakes Region

Adam Smith

Northeast Region

Trevis Gigliotti

Exploring the Potential of the Hyperspectral Remote Sensing Data China Orbita Zhuhai-1 in Land Cover Classification

Caixia Li, Xiaoyan Xiong, Lin Wang, Yunfan Li, Jiaqi Wang, and Xiaoli Zhang

Abstract

Responding to the shortcomings of China's civil remote sensing data in land cover classification, such as the difficulty of data acquisition and the low utilization rate, we used Landsat-8, China Orbita Zhuhai-1 hyperspectral remote sensing (OHS) data, and Landsat-8 + OHS data combined with band (red, green, and blue) and vegetation index features to classify land cover using maximum likelihood (ML), Mahalanobis distance (MD), and support vector machine (SVM). The results show that Landsat-8 + OHS data have the highest classification accuracy in SVM, with an overall accuracy of 83.52% and a kappa coefficient of 0.71, and this result is higher than that of Landsat-8 images and OHS images separately. In addition, the classification accuracy of OHS images was higher than that of Landsat-8 images. The results of the study provide a reference for the use of civil satellite remote sensing data in China.

Introduction

Land cover classification plays an increasingly important role in today's world as a key component of land management and environmental monitoring. Understanding land cover dynamics is necessary for sustainable land use planning, forest change monitoring, desertification monitoring, and biodiversity conservation. Traditional land use classification primarily relies on field statistics and survey information, which is a labor-intensive approach and challenging to implement for short-term monitoring.

In this context, remote sensing technology can capture information on land use on a large scale and at a high frequency. Multispectral and high temporal and spatial resolution image data not only expand the availability of data but also improve the accuracy and efficiency of land use classification due to the advantages of wide coverage and long time period. Land cover classification is a methodology based on geographic information systems (GISs) and remote sensing technology to better understand and use the potential of land by dividing the surface into different categories or types. The emergence of cloud computing platforms like Google Earth Engine has made the task of processing large-scale remote sensing data and performing land use classification more feasible. These platforms provide powerful computing resources and data storage that can support land use monitoring and classification projects on a global scale. They provide a simple and convenient solution for processing complex and redundant data and make large-scale land use categorization in ecologically fragile zones possible. They play an increasingly important role in data preprocessing and environmental monitoring.

Caixia Li, Xiaoyan Xiong, Lin Wang, Yunfan Li, Jiaqi Wang, and Xiaoli Zhang are from the State Key Laboratory of Efficient Production of Forest Resources; the Beijing Key Laboratory of Precision Forestry, College of Forestry; and the Key Laboratory of Forest Cultivation and Protection, Ministry of Education, Beijing Forestry University (zhang-xl@263.net).

Corresponding author: Huan Yang (yanghuan1105@163.com)

Contributed by Prasad S. Thenkabail, March 20, 2024 (sent for review April 21, 2024; reviewed by Itiya Aneee, Pardhasaradhi Teluguntla).

In the past decades, land use classification techniques have been mainly based on automatic identification and classification of land cover types. In the early days, these methods relied heavily on manually specified rules and characteristics; with the increase in computing power and the rise of machine learning techniques, automated and semiautomated classification methods became more widely used. The increase in the number and performance of modern satellites and remote sensing platforms, as well as the development of cloud computing and big data processing, provide more opportunities and challenges for land use classification. There are supervised and unsupervised classification methods (Li *et al.* 2014). The difference between these two methods is whether they require the selection of labeled samples as the basis for classification (Phillips 2002). The most commonly used classifiers for supervised classification include support vector machines (SVMs), Mahalanobis distance (MD), and maximum likelihood (ML) (Melgani and Bruzzone 2004; Valožić 2014).

The Landsat images have the advantages of fast acquisition speed, large coverage, and high sharing degree and are widely used in land use classification (Jia *et al.* 2014; Poursanidis *et al.* 2015; Borràs *et al.* 2017; Sharma *et al.* 2018; Ying *et al.* 2019). The launch of domestic hyperspectral satellites has revealed the great potential of hyperspectral data in land use classification and farmland monitoring. A considerable body of research has been conducted in this field, leading to numerous findings and advancements (Jia and Richards 1999; Bruzzone and Prieto 2001; Abdi and Hashemi 2016). Hyperspectral remote sensing has become one of the most valuable data sources for land cover classification due to its exceptional spectral resolution (Waske *et al.* 2010; Yang *et al.* 2012). *Zhuhai-1* is a satellite developed and operated by China Zhuhai Satellite Technology Co., Ltd. (CAST) and is one of the representatives of Chinese commercial remote sensing satellites. In December 2018, China released the *Zhuhai-1* commercial space hyperspectral satellite data (Xi *et al.* 2019). The results of ecological utilization classification monitoring using *Zhuhai-1* remote sensing image data in mine areas have shown superiority in ecological monitoring and vegetation succession characteristics of reclaimed areas (Xie and Tong 2014; Zhang *et al.* 2021). On the one hand, because the launch of this satellite was relatively recent, there have been few studies on its data for applications such as classification and change monitoring. On the other hand, achieving high accuracy spectral resolution usually requires a large instantaneous field of view, which is one of the important reasons for limiting the accuracy of spatial resolution (Xu *et al.* 2018). Hyperspectral images have limited ability to distinguish between similar features, which affects the breadth and depth of their applications in remote sensing (Jiang *et al.* 2019). Currently, further research is needed on the fusion of hyperspectral and multispectral information for classification (Lv and Wang 2020).

In this study, we used *Landsat-8*, *Orbita Zhuhai-1* hyperspectral remote sensing (OHS) images, and combined *Landsat-8* + OHS data to apply the ML, MD, and SVM methods of land cover classification.

Photogrammetric Engineering & Remote Sensing
Vol. 90, No. 10, October 2024, pp. 611–619.
0099-1112/22/611-619

© 2024 American Society for Photogrammetry
and Remote Sensing
doi: 10.14358/PERS.24-00034R2

**PEER-REVIEWED CONTENT
IS ONLY AVAILABLE TO
ASPRS MEMBERS AND SUBSCRIBERS**

**FOR MORE INFORMATION VISIT
[MY.ASPRS.ORG](https://my.asprs.org)**

**PEER-REVIEWED CONTENT
IS ONLY AVAILABLE TO
ASPRS MEMBERS AND SUBSCRIBERS**

**FOR MORE INFORMATION VISIT
MY.ASPRS.ORG**

**PEER-REVIEWED CONTENT
IS ONLY AVAILABLE TO
ASPRS MEMBERS AND SUBSCRIBERS**

**FOR MORE INFORMATION VISIT
[MY.ASPRS.ORG](https://my.asprs.org)**

**PEER-REVIEWED CONTENT
IS ONLY AVAILABLE TO
ASPRS MEMBERS AND SUBSCRIBERS**

**FOR MORE INFORMATION VISIT
[MY.ASPRS.ORG](https://my.asprs.org)**

**PEER-REVIEWED CONTENT
IS ONLY AVAILABLE TO
ASPRS MEMBERS AND SUBSCRIBERS**

**FOR MORE INFORMATION VISIT
[MY.ASPRS.ORG](https://my.asprs.org)**

**PEER-REVIEWED CONTENT
IS ONLY AVAILABLE TO
ASPRS MEMBERS AND SUBSCRIBERS**

**FOR MORE INFORMATION VISIT
[MY.ASPRS.ORG](https://my.asprs.org)**

**PEER-REVIEWED CONTENT
IS ONLY AVAILABLE TO
ASPRS MEMBERS AND SUBSCRIBERS**

**FOR MORE INFORMATION VISIT
[MY.ASPRS.ORG](https://my.asprs.org)**

- Phillips, S. 2002. Reducing the computation time of the Isodata and K-means unsupervised classification algorithms. *IEEE International Geoscience & Remote Sensing Symposium* 3: 1627–1629.
- Poursanidis, D., N. Chrysoulakis and Z. Mitraka. 2015. *Landsat 8 vs. Landsat 5: A comparison based on urban and peri-urban land cover mapping. International Journal of Applied Earth Observation and Geoinformation* 35(1): 259–269.
- Rasti, B., M. O. Ulfarsson and J. R. Sveinsson. 2016. Hyperspectral feature extraction using total variation component analysis. *IEEE Transactions on Geoscience and Remote Sensing* 54: 6976–6985.
- Richards, J. A., ed. 2013. Supervised classification techniques. In *Remote Sensing Digital Image Analysis: An Introduction*. Berlin/Heidelberg, Germany: Springer.
- Sharma, J., R. Prasad, V. N. Mishra, V. P. Yadav and R. Bala. 2018. Land use and land cover classification of multispectral *Landsat-8* satellite imagery using discrete wavelet transform. *International Archives of the Photogrammetry, Remote Sensing and Spatial Information Sciences* 5: 703–721.
- Silveira, E. M. O., I. T. Bueno, F. W. Acerbi-Junior, J. M. Mello, J. R. S. Scolforo and M. A. Wulder. 2018. Using spatial features to reduce the impact of seasonality for detecting tropical forest changes from *Landsat* time series. *Remote Sensing* 10: 808.
- Sun, Y. H., H. Z. Ren, T. Y. Zhang, C. Y. Zhang and Q. M. Qin. 2018. Crop leaf area index retrieval based on inverted difference vegetation index and NDVI. *IEEE Geoscience and Remote Sensing Letters* 15: 1662–1666.
- Tan, K., X. Wang, C. Niu, F. Wang, P. J. Du, D. X. Sun, J. Yuan and J. Zhang. 2021. Vicarious calibration for the AHSI instrument of *Gaofen-5* with reference to the CRCS Dunhuang test site. *IEEE Transactions on Geoscience and Remote Sensing* 59: 3409–3419.
- Valozić, L. 2014. Land cover classification of urban and peri-urban areas using object-oriented analysis of multispectral imagery. *Hrvatski Geografski Glasnik* 76(2): 27–38.
- Waske, B., S. van der Linden, J. A. Benediktsson, A. Rabe and P. Hostert. 2010. Sensitivity of support vector machines to random feature selection in classification of hyperspectral data. *IEEE Transactions on Geoscience and Remote Sensing* 48(7): 2880–2889.
- Xi, Y. B., C. Y. Ren, Z. M. Wang, S. Q. Wei, J. L. Bai, B. Zhang, H. X. Xiang and L. Chen. 2019. Mapping tree species composition using OHS-1 hyperspectral data and deep learning algorithms in Changbai mountains, Northeast China. *Forests* 10: 818.
- Xie, H. and X. Tong. 2014. A probability-based improved binary encoding algorithm for classification of hyperspectral images. *IEEE Journal of Selected Topics in Applied Earth Observations and Remote Sensing* 7(6): 2108–2118.
- Xu, X., J. Li, Y. Zhang and S. Li. 2018. A subpixel spatial–Spectral feature mining for hyperspectral image classification, *2018 IEEE International Geoscience and Remote Sensing Symposium*, 22–27 July 2018, Valencia, Spain, pp. 8476–8479.
- Yang, H., Q. Du and G. Chen. 2012. Particle swarm optimization-based hyperspectral dimensionality reduction for urban land cover classification. *IEEE Journal of Selected Topics in Applied Earth Observations and Remote Sensing* 5(2): 544–554.
- Ying, L., C. Chao, G. Hailing and C. Yanli. 2019. Remote sensing monitoring of ecological environment based on *Landsat* data. *IOP Conference Series: Earth and Environmental Science* 310(5): 052061.
- Zhang, C., Z. Gong, H. Qiu, Y. Zhang and D. Zhou. 2021. Mapping typical salt-marsh species in the Yellow River Delta wetland supported by temporal–spatial–spectral multidimensional features. *Science of the Total Environment* 783: 147061.

In-Press Articles

Morphology-Based Feature Extraction Network for Arbitrary-Oriented SAR Vehicle Detection

Ting Chen and Xiaohong Huang

Spatial-Spectral Middle Cross-Attention Fusion Network for Hyperspectral Image Superresolution

Xiujuan Lang, Tao Lu, Yanduo Zhang, Junjun Jiang, and Zixiang Xiong

Machine Learning and New-Generation Spaceborne Hyperspectral Data Advance Crop Type Mapping

Itiya Aneece, Prasad S. Thenkabail, Richard McCormick, Hairiti Alifu, Daniel Foley, Adam J. Oliphant, Pardhasaradhi Teluguntla

A Variable-Iterative Fully Convolutional Neural Network for Sparse Unmixing

Fanqiang Kong, Zhijie Lv, Kun Wang, Xu Fang, Yuhan Zheng, and Shengjie Yu

Remote Sensing Tailing Pond Image–Detection Method Based on YOLOv8-RVSW

Zhengjun Dang and Kun Li

Monitoring LULC Changes in Babil Province for Sustainable Development Purposes Within the Period 2004–2023

Hayder Hameed Jassoom and Rabab Saadoon Abdoon

The layman's perspective on technical theory and practical applications of mapping and GIS



MAPPING MATTERS

YOUR QUESTIONS ANSWERED

by **Qassim Abdullah, Ph.D., PLS, CP**
Woolpert Vice President and Chief Scientist

- Have you ever wondered about what can and can't be achieved with geospatial technologies and processes?
- Would you like to understand the geospatial industry in layman's terms?
- Have you been intimidated by formulas or equations in scientific journal articles and published reports?
- Do you have a challenging technical question that no one you know can answer?



If you answered “YES” to any of these questions, then you need to read Dr. Qassim Abdullah's column, **Mapping Matters**.

In it, he answers all geospatial questions—no matter how challenging—and offers accessible solutions.

Send your questions to Mapping_Matters@asprs.org

To browse previous articles of Mapping Matters, visit <http://www.asprs.org/Mapping-Matters.html>

“Your mapping matters publications have helped us a lot in refining our knowledge on the world of Photogrammetry. I always admire what you are doing to the science of Photogrammetry. Thank You Very much! the world wants more of enthusiast scientists like you.”

“I read through your comments and calculations twice. It is very clear understandable. I am Honored there are experienced professionals like you, willing to help fellow members and promote knowledge in the Geo-Spatial Sciences.”

YOUR COMPANION TO SUCCESS

Teacher-Student Prototype Enhancement Network for a Few-Shot Remote Sensing Scene Classification

Ye Zhu, Shanying Yang, and Yang Yu

Abstract

Few-shot remote sensing scene classification identifies new classes from limited labeled samples where the great challenges are intraclass diversity, interclass similarity, and limited supervision. To alleviate these problems, a teacher-student prototype enhancement network is proposed for a few-shot remote sensing scene classification. Instead of introducing an attentional mechanism in mainstream studies, a prototype enhancement module is recommended to adaptively select high-confidence query samples, which can enhance the support prototype representations to emphasize intraclass and interclass relationships. The construction of a few-shot teacher model generates more discriminative predictive representations with inputs from many labeled samples, thus providing a strong supervisory signal to the student model and encouraging the network to achieve accurate classification with a limited number of labeled samples. Extensive experiments of four public datasets, including NWPU-remote sensing image scene classification (NWPU-RESISC45), aerial image dataset (AID), UC Merced, and WHU-RS19, demonstrate that this method achieves superior competitive performance than the state-of-the-art methods on five-way, one-shot, and five-shot classifications.

Introduction

Remote sensing scene classification (RSSC) is one of the most basic tasks in remote sensing image processing, which aims to assign semantic labels to each remote sensing scene (Chaib *et al.* 2017). The RSSC has been widely used in various fields, such as disaster detection (Longbotham *et al.* 2012), resource planning (Zhu *et al.* 2021), and environmental monitoring (Tian *et al.* 2019).

In recent years, deep-learning methods have been widely used in RSSC tasks because of their excellent feature extraction capabilities (Cheng, Xu *et al.* 2021); the core idea is to use deep neural networks such as convolutional neural networks (Zhang *et al.* 2016), deep belief network (Chen *et al.* 2015), and recurrent neural networks (Zaremba *et al.* 2014) for end-to-end feature extraction to achieve scene classification. However, these methods require a large amount of labeled data to train the network and often face overfitting in ungenerous labeled samples (Ma *et al.* 2019).

Annotating massive remote sensing images is time-consuming and labor-intensive work. To reduce the reliance on data annotation, more researchers are paying more attention to a few-shot RSSC (Fei-Fei *et al.* 2006), where the meta-learning methods have achieved remarkable success (Wang *et al.* 2023). Zhang *et al.* (2020) applied the cosine distance with learnable scale parameters to optimize the classifier in the metric space based on a meta-learning framework. To reduce the background noise interference, which improves classification ability, researchers proposed a self-attention-based feature encoder (Zeng *et al.* 2021). Xing, Ma *et al.* (2022) designed and optimized the feature

extraction ability of the network and trained a great linear classifier to obtain advanced performance.

Two major challenges persist for a few-shot RSSC: intraclass diversity and interclass similarity and a supervision-limited problem under a sample-limited scenario. Compared with natural images, the distribution of ground objects in remote sensing images is complex and varied, which makes the diversification of objects in scene images of the same semantic category result in intraclass diversity. Similarly, scene images of different semantic categories may have a high degree of similarity (Figure 1). Typically, the classification loss of the query set on the classifier is the primary supervision, which determines how the network should learn prior knowledge from the support set. However, the few-shot query samples do not provide sufficient supervision for the network, whereas the larger the number of support shots, the more limited supervision of the query set will cause a drastic decrease in the effectiveness of meta-learning (Ye *et al.* 2022).

To alleviate these two problems, a teacher-student prototype enhancement network (TSPE-Net) for a few-shot RSSC is proposed; the network has a flexible few-shot learning capability while generating accurate decision boundaries (Figure 2). A prototype enhancement module (PEM) is suggested to address the challenge of intraclass diversity and interclass similarity in remote sensing images; this module performs learnable prototype enhancement by adaptively selecting high-confidence query samples instead of introducing an attention mechanism (Chen, Li *et al.* 2023; Xia *et al.* 2023). To address the problem of limited supervision, a few-shot teacher model (FS-TM) is introduced to construct the teacher-student framework, which generates more accurate feature representations to achieve powerful classification capabilities using several labeled support samples. Furthermore, potential information is transferred from the teacher model to the student model through knowledge distillation, guiding the student model to predictively classify the query set in a manner similar to the powerful classifiers of the teacher model.

The contribution of this work is summarized as follows. A flexible PEM is designed to adaptively select high-confidence query samples, which can effectively capture the intraclass and interclass relationships of remote sensing images. A teacher-student model that implicitly breaks out of the shots set up to optimize the prediction between teacher and student models is introduced; the teacher-student model guides the student model to achieve accurate classification under limited samples. Finally, extensive experiments on four public remote sensing scene datasets demonstrate that the proposed method achieves superior competitive performance than mainstream few-shot RSSC methods.

Ye Zhu, Shanying Yang, and Yang Yu are with the School of Artificial Intelligence, Hebei University of Technology, Tianjin 300401, China.

Corresponding author: Yang Yu (yuyang@hebut.edu.cn)

Contributed by Alper Yilmaz, October 17, 2023 (sent for review May 10, 2024; reviewed by Alper Yilmaz).

Photogrammetric Engineering & Remote Sensing
Vol. 90, No. 10, October 2024, pp. 621–630.

0099-1112/22/621-630

© 2024 American Society for Photogrammetry
and Remote Sensing

doi: 10.14358/PERS.23-00077R2

**PEER-REVIEWED CONTENT
IS ONLY AVAILABLE TO
ASPRS MEMBERS AND SUBSCRIBERS**

**FOR MORE INFORMATION VISIT
[MY.ASPRS.ORG](https://my.asprs.org)**

**PEER-REVIEWED CONTENT
IS ONLY AVAILABLE TO
ASPRS MEMBERS AND SUBSCRIBERS**

**FOR MORE INFORMATION VISIT
[MY.ASPRS.ORG](https://my.asprs.org)**

**PEER-REVIEWED CONTENT
IS ONLY AVAILABLE TO
ASPRS MEMBERS AND SUBSCRIBERS**

**FOR MORE INFORMATION VISIT
[MY.ASPRS.ORG](https://my.asprs.org)**

**PEER-REVIEWED CONTENT
IS ONLY AVAILABLE TO
ASPRS MEMBERS AND SUBSCRIBERS**

**FOR MORE INFORMATION VISIT
[MY.ASPRS.ORG](https://my.asprs.org)**

**PEER-REVIEWED CONTENT
IS ONLY AVAILABLE TO
ASPRS MEMBERS AND SUBSCRIBERS**

**FOR MORE INFORMATION VISIT
[MY.ASPRS.ORG](https://my.asprs.org)**

**PEER-REVIEWED CONTENT
IS ONLY AVAILABLE TO
ASPRS MEMBERS AND SUBSCRIBERS**

**FOR MORE INFORMATION VISIT
[MY.ASPRS.ORG](https://my.asprs.org)**

**PEER-REVIEWED CONTENT
IS ONLY AVAILABLE TO
ASPRS MEMBERS AND SUBSCRIBERS**

**FOR MORE INFORMATION VISIT
[MY.ASPRS.ORG](https://my.asprs.org)**

**PEER-REVIEWED CONTENT
IS ONLY AVAILABLE TO
ASPRS MEMBERS AND SUBSCRIBERS**

**FOR MORE INFORMATION VISIT
[MY.ASPRS.ORG](https://my.asprs.org)**

**PEER-REVIEWED CONTENT
IS ONLY AVAILABLE TO
ASPRS MEMBERS AND SUBSCRIBERS**

**FOR MORE INFORMATION VISIT
[MY.ASPRS.ORG](https://my.asprs.org)**

Bank Line Extraction by Integration of Orthoimages and Lidar Digital Elevation Model Using Principal Component Analysis and Alpha Matting

Sagar S. Deshpande

Abstract

Riverbank lines change over time, causing loss of land and property. Accurate mapping of riverbank lines is essential for restoration and preservation. This paper presents a method to map riverbank lines by combining georeferenced orthoimages and lidar digital elevation model (DEM). This method uses the properties that lidar can provide elevations under trees and open water edges are visible in orthoimages to extract the planimetric locations of bank lines. The orthoimage pixels with less than 0.15% slope on the DEM were replaced by water pixels. Principal component analysis (PCA) was conducted using DEM, slope, and orthoimage bands. Training data of river body and the background were identified manually on the first three component images. An alpha matting-based method was implemented using the training data to extract the bank lines. Bankline using a value of 50% probability were statistically and visually better when compared to the manual bank lines.

Introduction

The boundaries of water bodies such as oceans, seas, lakes, and rivers change over time due to various socioenvironmental factors. Kummur *et al.* (2011) stated that around half of the world's population lives within 3 km of a freshwater body, and 90% lives within 10 km. Hence, periodic and accurate mapping of shorelines or bank lines is important for the existing and future population along with the water bodies. Additionally, river waters are used for irrigation, domestic use, transportation, power generation, and recreational activities. Rivers also provide protection against floods and provide food and habitat for several marine animals. Rivers play a very important role in the water cycle by draining surface water. Thus, mapping rivers can provide a better understanding of changes in the riverbank lines over time.

Definition of Riverbank Lines

A schematic view of a river cross-section is shown in Figure 1. The main channel of a perennial river carries the water for the most part of the year. The changes in the water level are affected by the rate of flow at any given time and the bank slopes. The instantaneous water surface is the water level at the time of data acquisition. The intersection of this water surface with the riverbanks defines the bank line location of the river. Gentle slopes of banks can change the location of bank lines significantly over time as compared to steep slopes. Overall, the river runoff, sediments transported in a river, and the geometry of a river can cause erosion of the riverbanks. Riverbank erosion is the second key process in fluvial dynamics, which has a greater influence on several physical, ecological, and socioeconomic issues (Rinaldi *et al.* 2013).

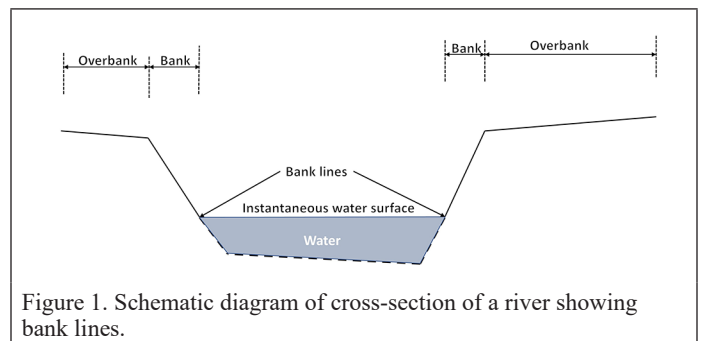


Figure 1. Schematic diagram of cross-section of a river showing bank lines.

Historically, bank lines have been mapped using conventional field survey methods that were time-consuming and not detailed. Over the past two decades, lidar data have been used for coastal and riverine land-water boundary mapping (Deshpande 2017). Several studies have integrated spatial data sets from various sensors such as single photon lidar, aerial imagery, hyperspectral imagery, etc., to determine the bank lines of water bodies.

In this paper, a new method based on the alpha matting process is presented for the determination of riverbank shorelines by combining orthoimage and lidar digital elevation model (DEM). The main objectives are to use the complementary properties of both imagery and lidar for the accurate identification of riverbank lines. Additionally, this method provides a probabilistic approach to determine the riverbanks.

This paper is organized into six sections. Following this introduction section, the second section reviews the latest development in the field of lidar and aerial imaging technology. This section also provides a summary of research works pertinent to bank lines and shoreline extraction using different geospatial data sets. The third section describes the data used in this research. The fourth section describes the methodology developed to integrate aerial images and lidar to extract riverbank lines. The fifth section describes and discusses the results. The last section provides concluding remarks for the presented methodology and its limitations. This section also discusses avenues for future research.

Orthoimages and lidar elevation data are the two important data sets that are extensively used in the geospatial domain. Orthoimages are created by removing the effects of tilt and relief from aerial images. Unlike the aerial photo, the orthoimages have a uniform scale and can be laid directly over other maps. As shown in Figure 2, the river surface can be covered by nearby trees, thereby blocking the view to the riverbank lines.

Sagar S. Deshpande is with Dewberry.

Corresponding author: Sagar S. Deshpande (sagard79@gmail.com)

Contributed by Filiz Sunar, October 6, 2021 (sent for review February 22, 2022; reviewed by Mustafa Zeybek).

Photogrammetric Engineering & Remote Sensing
Vol. 90, No. 10, October 2024, pp. 631–638.
0099-1112/22/631–638

© 2024 American Society for Photogrammetry
and Remote Sensing
doi: 10.14358/PERS.21-00078R2

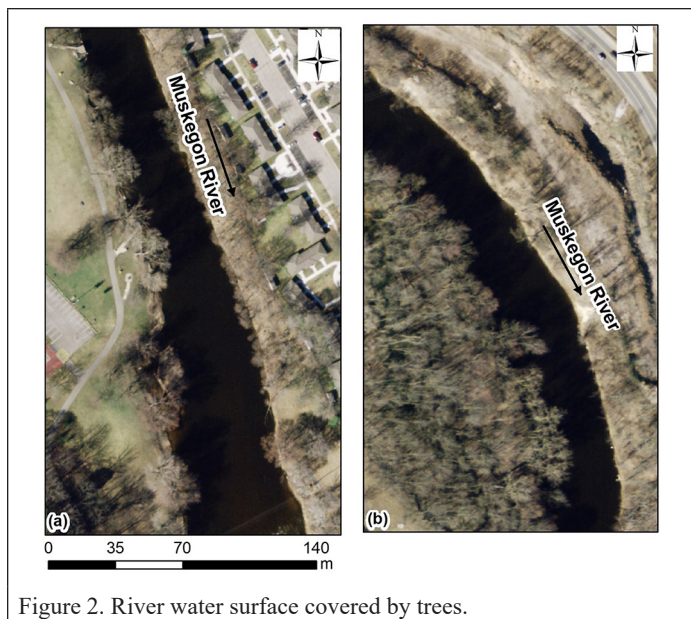


Figure 2. River water surface covered by trees.

Lidar is an active sensor that collects topographic information. Lidar sensors can collect points below a tree canopy because its pulses can pass through the gaps in the canopy (Deshpande and Yilmaz 2017). Typically, lidar data are used to create a bare ground surface by removing vegetation, buildings, and other man-made structures. Fewer lidar points are collected over water surfaces, which can result in an unnatural DEM surface. Hence, a hydro-flattened DEM (U.S. Geological Survey 2024) is created using lidar data that shows water surfaces as they would occur in nature, i.e., the river surfaces slope downstream, and lakes and ponds have a constant elevation (Deshpande and Yilmaz 2017). Both the orthoimages and lidar data have been used in numerous studies to extract features relevant to civil engineering.

Breakline Mapping Using Aerial Photos and Lidar

Breaklines represent edges in geospatial data with a change in elevation (Deshpande 2013). They represent significant terrain features like lakes, rivers, or cliffs that cause a change in slope. In lidar data, a significant change in elevation would be defined using a breakline. For example, the edge of a building in lidar data would be a breakline. A change in elevation from the river water surface to the ground would be represented as a breakline. In an aerial image, these breaklines are typically located with changes in image contrast. For example, the riverbank line as shown in Figure 2 will be a breakline. Various studies have reported extraction of breaklines using aerial photos and/or lidar data as discussed below.

Grau *et al.* (2021) used images acquired from an unmanned aerial vehicle (UAV) to estimate channel boundary within grazed riparian pastures. Two methods, the slope gradient (SG) and vertical slope position (VSP), were used in their study. They applied the same methods to other elevation products, such as low-resolution DEM and two different resolution lidar data sets for comparison. This study found that the UAV-based DEM could be used to identify steep banks. BhavanGowda *et al.* (2021) proposed an innovative and practical method of predicting the changes in the coastline by analyzing the images recorded through Google earth. Backes *et al.* (2020) investigated monitoring the morphology of a frequently changing glacial stream using high-resolution topographic models created from UAV-based photogrammetry and lidar. This study reported a highly dynamic character of the riverbed in terms of relocation of river channels and failure of riverbanks due to lateral undercutting. Myers *et al.* (2019) evaluated streambank line erosion using three data acquisition techniques: erosion pins, total stations, and laser scanning. Nine sites, each with an 18-m section of stream, were selected for their study. Their study concluded that the application of each technique is dependent on the site conditions and project goals. Ngadiman *et al.* (2021), Hamshaw *et al.* (2019), and

Duró *et al.* (2018) applied structure-from-motion (SfM) techniques to imagery acquired from UAV-based platform to measure bank erosion processes. Duró *et al.* (2018) studied along a 1.2-km river reach. Eight UAV sessions were conducted to identify effective UAV flights. This study reported that an oblique perspective with eight overlapping photos and 20 m of cross-sectional ground control distribution was sufficient to achieve 3-cm accuracy. Deshpande and Yilmaz (2017) presented a methodology to extract riverbank lines from lidar points to create a hydro-flattened DEM. A modified approach was presented by Deshpande (2017) to extract riverbank lines from single photon lidar data to create a hydro-flattened DEM. Several other studies (Höfle *et al.* 2009; Vandromme *et al.* 2017; Mason and Mohrig 2018; Wolter *et al.* 2021) reported the use of lidar data to monitor changes along rivers using lidar data. This part of the literature review highlighted the importance of riverbank mapping using aerial and UAV-based imagery and lidar data alone. The subsequent subsection discusses the research by combining data from more than one sensor.

Data Integration

Various remote sensing data sets, depending on their sensor, have different properties. For example, aerial images provide an aerial view, and lidar data provide elevation on the ground. Elevation information under a tree canopy can be obtained from lidar data. Researchers have used various properties of sensors to extract pertinent ground features.

Cal (2020) presented an object-based method to extract buildings using principal component analysis (PCA) of lidar and aerial photos. Five experiments were conducted using different combinations of lidar derivatives and aerial photos bands in a PCA. This research reported that a combination of lidar heights, RGB bands, and NIR bands produced the best result. Jayathunga *et al.* (2018) analyzed forest structures using lidar and aerial photos. A multivariate set that included three lidar metrics (95th percentile canopy height, canopy density, and surface area ratio) and one image was used to classify forest structure into structural complexity classes. Cluster analysis was able to identify six forest structural complexity classes including two low-complexity classes and four high-complexity classes. Choung (2014) reported a methodology to map different objects of levees using lidar and multispectral orthoimages. Levee crown, berm, sloped surfaces, and the eroded area were identified using multiple geometric analysis approaches. Additionally, spectral analysis approaches were used to identify major objects using orthoimages. Liu *et al.* (2009) used orthoimages to define the horizontal position of blufflines and extracted the elevation from lidar data. This method combined the properties of both data sets to produce accurate blufflines. Li *et al.* (2008) presented a rational model-based integration method to combine aerial and satellite images to produce an accurate shoreline. Legleiter (2012) developed and evaluated a hybrid approach to remote measurement of river morphology by combining lidar topography and bathymetry. Fernández *et al.* (2020) and Niculiță *et al.* (2020) presented methods using aerial photographs and airborne lidar data available from public database servers to identify and quantify gully erosion. Chen *et al.* (2004) proposed a two-part scheme to model buildings using lidar and Quickbird satellite imagery.

Based on the literature review, it can be summarized that the properties of orthoimages and lidar can be combined to extract linear features. Such a method will use the elevation information from the lidar data, which is also available under a tree canopy, and will use visible information from orthoimages. Based on these properties, the goal of this paper is to present a method to combine these two properties to extract riverbank lines using PCA and the alpha matting process. This method would provide the probable shoreline location based on the combined information from the lidar and orthoimagery.

Alpha Matting

Alpha matting is a process of extracting a foreground object from an image along with an opacity estimate for each pixel covered by the object (Levin *et al.* 2008). It is an invaluable tool used in image editing, video production, and special effects in motion pictures. Various alpha matting processes have been proposed by several researchers (Grady *et*

al. 2005; Levin *et al.* 2008; Rhemann *et al.* 2008; Gastal and Oliveira 2010; He *et al.* 2011). An example of the alpha matting process is shown in Figure 3a, with an original image that has a tower and blue sky. The tower has various color sections throughout its height. Figure 3b shows the manual identification of background and foreground pixels as shown in black and white colors. Figure 3c shows the output after the alpha matting process. The pixels in this image have α values ranging from 0 to 1. The α value represents the probability of a pixel being part of either the foreground or the background areas (Grady *et al.* 2005). It can be noted that near the top edge of the tower that some

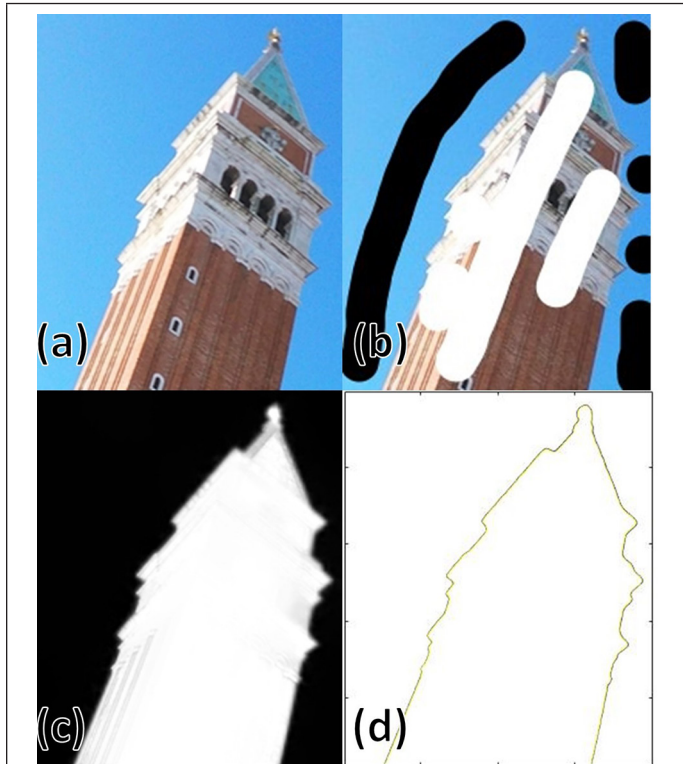


Figure 3. Alpha matting example. (a) Original image of the tower. (b) Background and foreground identification. (c) Alpha value map. (d) Contour of $\alpha = 0.5$.



Figure 4. Overview of the orthoimages showing the river and the neighboring areas. (a) Region 1: semiurban area. (b) Region 2: rural area.

pixels are gray colored, showing a lower probability. Figure 3d shows a 50% probability contour using $\alpha = 0.5$ that determined the outline of the tower. It can be noted that different values of α would produce different results.

In the proposed methodology, the alpha matting process proposed by Levin *et al.* (2008) was adapted to extract the riverbank lines using lidar DEM and orthoimages. This method is explained later under “Methodology.”

Data Used

The orthophotos and lidar-derived DEM used in this study are shown in Figure 4. The river centerlines of the two regions were approximately 2.2 km each. The first region was selected in a semiurban area where the riverbanks were not significantly covered by vegetation. The second region was selected in a rural area where the riverbanks were significantly covered by vegetation. The details of the data sets are explained in the following section.

Orthoimages

The aerial images for the orthoimages were acquired using two Leica ADS40 imaging sensors. The orthophoto mosaics were produced at 0.3048-m (1-foot) resolution. The aircraft used were a twin-engine Beechcraft King Air E90 and twin-engine Cessna 402C. The data were projected using the State Plane Michigan South, horizontal datum – North American Datum of 1983 (NAD83 2011). A horizontal accuracy of 0.79 m was reported by the vendor. Figure 4 shows the overview of the two study areas used in this paper. The river lengths were approximately 2.2 km in both regions.

Lidar-based DEM

An overview of the lidar DEM data sets used in this study is shown in Figure 5.

The lidar data used in this study were acquired in the fall of 2014. These data were captured using a Leica ALS70 lidar instrument an integrated IPAS20 GPS/INS system mounted within an Aero Commander twin-engine airplane. About 2 million points existed within a tile of 0.58-km² area, resulting in an average point density of 3.4 points/m². The data were projected using the State Plane Michigan South, horizontal datum – North American Datum of 1983 (NAD83 2011). The elevations were with reference to the North American Vertical Datum of 1988 (NAVD88) using the latest geoid (Geoid12a). A horizontal accuracy of 1 m was reported by the vendor. The

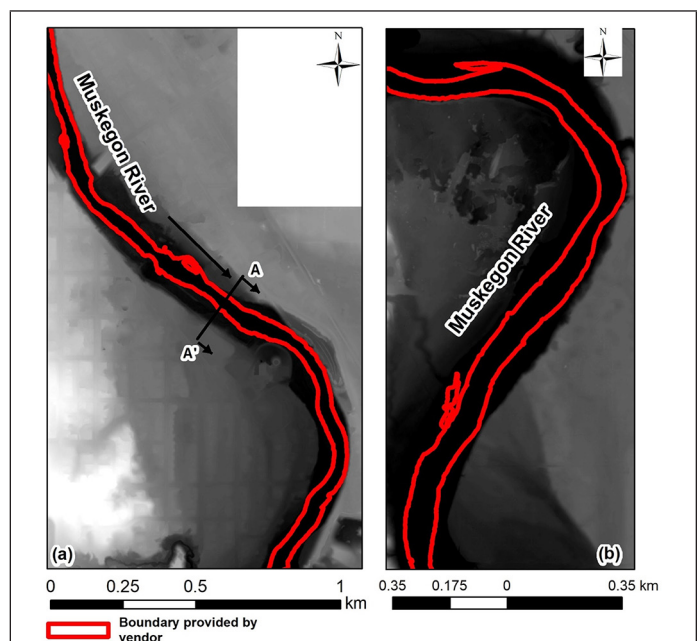


Figure 5. Overview of the lidar data and the bank lines provided by the vendor. (a) Region 1. (b) Region 2.

hydro-flattened DEM created by the vendor using the lidar point cloud was used in this study. The resolution of the DEM was 0.91 m (3 feet). The orthoimages were down sampled to 0.91-m pixel size to match the DEM resolution. The proposed methodology to use these data sets to extract bank lines is explained in the next section.

Methodology

Figure 6 shows the overview of the new methodology proposed to extract riverbank shoreline by integrating orthophotos and lidar DEM. The methodology is based on the use of georeferenced orthoimages and lidar DEM as explained below.

Lidar DEM

As explained in the data description section, the hydro-flattened DEMs (Figure 5) used in this study were created by the vendor using the bare ground points classified. Figure 7a shows an elevation profile along the cross-section AA' as identified in Figure 5b. This figure shows the water surface of the river, the bank lines, and the overland. It can be

observed that the water surface elevation was lower than the rest of the terrain in each area. Because the DEM was hydro-flattened, the water surface was even from bank to bank, having almost no slope. This was an important spatial property of the water surface that was used in this study. A slope map was created as explained in the next section.

Slope Map

A percentage slope raster was created using the lidar DEM. The slope value profile along the cross-section AA' is shown in Figure 7b. It can be noted that the slope values within the banks were near zero. This was one of the important spatial properties observed in the slope raster for the water surface. Upon close inspection, slope values of less than 0.0015 were observed in the water areas of the slope raster. Close inspection of the entire slope map also revealed isolated land cells with slope values close to zero. To remove these isolated land cells, a median filter was implemented on the slope raster using a size kernel so that each central pixel was replaced by a median slope value. This process eliminated most of the land cells with slope values close to zero.

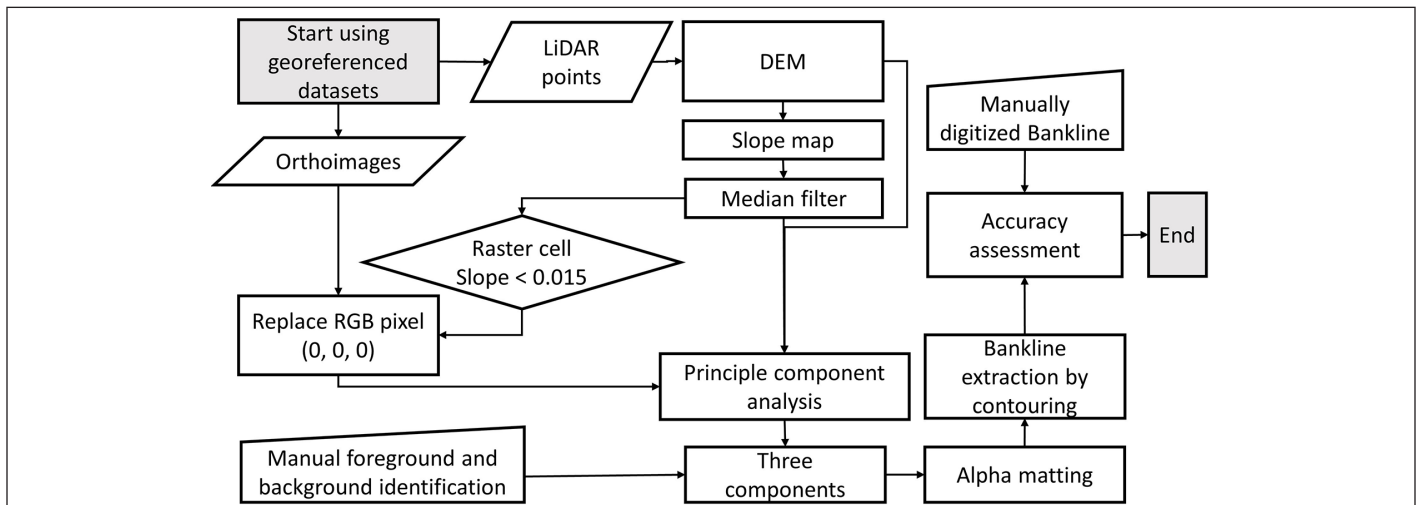


Figure 6. Overview of the methodology to extract riverbank shorelines using lidar digital elevation model (DEM) and orthoimages.

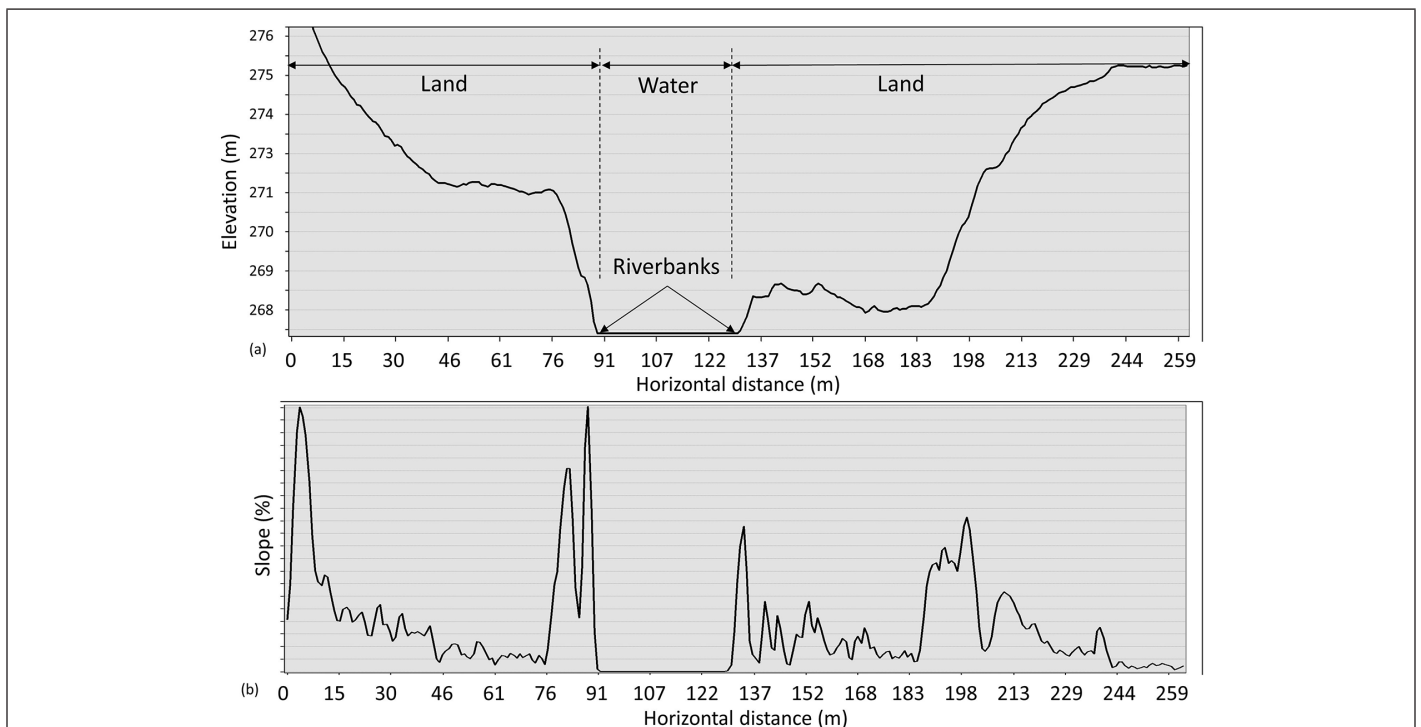


Figure 7. (a) Elevation profile along the cross-section AA' shown as shown in Figure 4b. (b) Slope profile along the cross-section AA'.

Color Image

Figure 4 shows the orthoimages used in this study. The following points were observed about the orthoimages:

- The water surface was represented by darker pixels (close to zero) in the red, green, and blue bands.
- The bank lines that were not covered by trees were clearly identifiable.
- Upon close visual inspection, it was noticed that the riverbanks were covered by trees, thereby making identification of banks difficult. A zoomed-in view of the river is shown in Figure 8a that shows the trees covering the bank lines.

The trees that covered the riverbanks would result in erroneous bank lines. Thus, it was necessary to modify the orthoimages that covered the river surfaces using the lidar DEM. The property of the median slope surface created using the lidar DEM showed values less than 0.15% for the water surface. Using this criterion, the image pixels with a corresponding median slope pixel value of less than 0.15% were replaced by R = 0, G = 0, and B = 0 to resemble the water pixels. A zoomed-in view of the revised orthoimage is shown in Figure 8b showing that the tree pixels were modified to be represented as water pixels.

At this stage, a three-band orthoimage, lidar elevation raster, and a median slope raster of the study areas were available. Each of these layers had property that would identify the river surface and bank lines. These layers were processed using the PCA, as described in the next section.

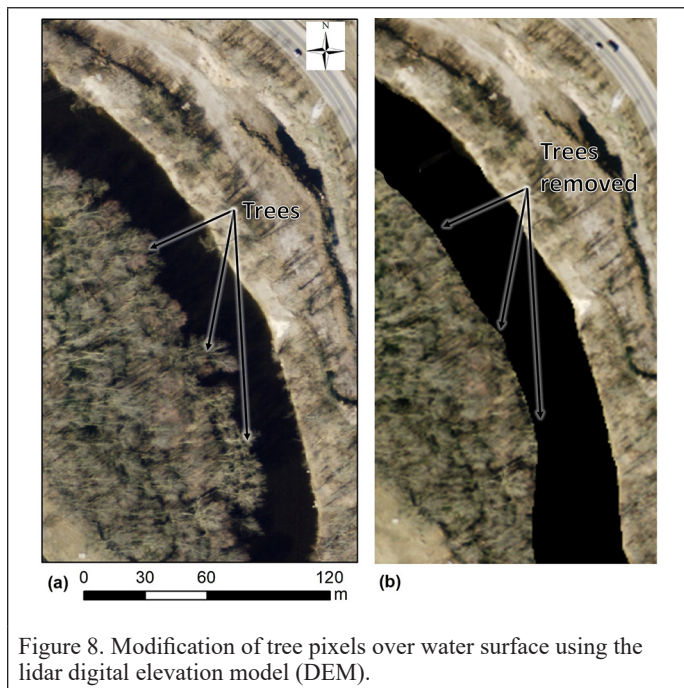


Figure 8. Modification of tree pixels over water surface using the lidar digital elevation model (DEM).

Principal Component Analysis

PCA is commonly used for dimensionality reduction by projecting each data point onto only the first few principal components to obtain lower-dimensional data while preserving as much of the data's variation as possible. In the current study, PCA was implemented on the five layers: red, green, blue orthoimage bands, lidar elevations, and the slope image. A variance-covariance matrix for the five bands was created, and the eigen vectors and eigen values were determined to compute the principal components of the data. These principal components are a linear combination of the initial data and are uncorrelated. The first principal component can equivalently be defined as a direction that maximized the variance of the projected data. The principal components were reshaped to the original image shape and normalized from 0 to 255. These five component images for region 1 are shown in Figure 9.

The eigen values expressed in percentages state the information retained in each principal component. From Table 1 it can be noticed that the first three components retained 98% of information. Thus, these three components were used in the next step of alpha matting.

Table 1. Principal component analysis (PCA) results for the two study regions.

Principal component	Region 1	Region 2
1	82.6	76.4
2	14.2	20.0
3	1.8	2.2
4	1.1	0.9
5	0.3	0.6

Alpha Matting

Alpha matting is the process of extracting a foreground object from an image along with an opacity estimate for each pixel covered by the object (Levin *et al.* 2008). It is an invaluable tool used in image editing, video production, and special effects in motion pictures. This method typically assumes that every pixel I_i in a digital image is a linear combination of a foreground color F_i and a background color B_i :

$$I_i = \alpha_i F_i + (1 - \alpha_i) B_i \quad (1)$$

Equation 1 is known as the composition equation. For regular images, F and B are not constrained to a particular subset of values (Gastal and Oliveira 2010), resulting in all variables on the right-hand side of Equation 1 being unknowns. This makes the problem of computing an alpha matte considerably difficult. Due to the highly ill-posed nature of the problem, additional constraints in the form of user input as scribbles are required. This user-supplied information identifies pixels for which the α value is known to be 1 (foreground) or 0 (background).

As discussed in the literature review section, several alpha matting processes have been proposed by different researchers. In this work, we use the method proposed by Levin *et al.* (2008) because it provided a

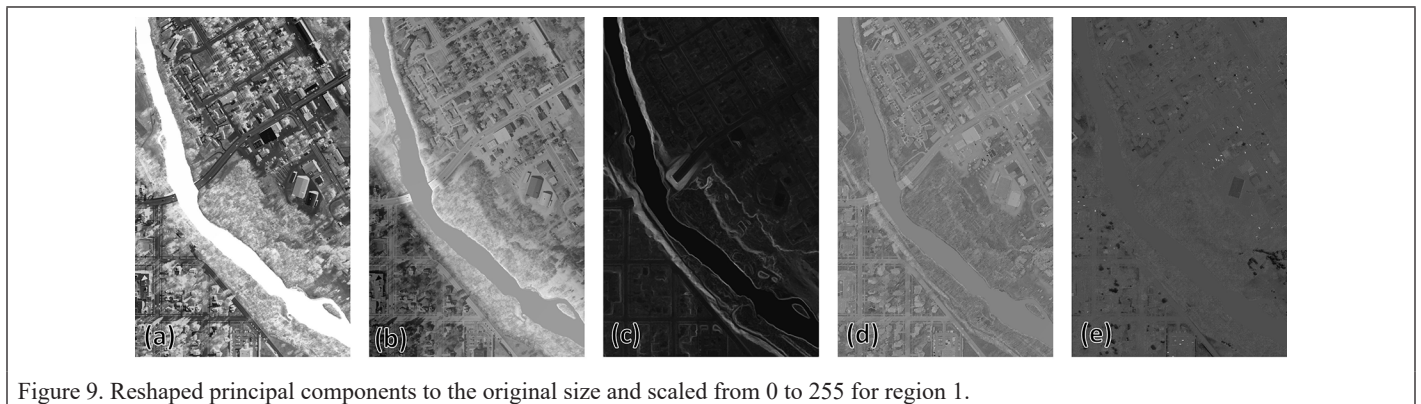


Figure 9. Reshaped principal components to the original size and scaled from 0 to 255 for region 1.

simple intuitive preview of optional outputs, allowing control of the outcome in the fractional parts of the matte. This method also allowed control of the number of eigenvectors. The alpha matting process involves three steps: computing the Laplacian matrix, computing the matting components, and grouping the matting components (Levin *et al.* 2008).

The first three principal component images were combined to create a color image as shown in Figure 10a. It can be seen that the river areas are more homogeneous, whereas the remaining regions consist of several variations. The river was assigned as foreground, and the remaining area was assigned as background using scribbles as shown in Figure 10b.

Because the alpha matting method is sensitive to the scribbles, processing a larger image would require significantly more scribbles. An alternative method was to process smaller sections of the data. The entire data collection was divided into horizontal bands, each containing 200 rows and all columns. For the proposed approach, 40 matting components were extracted using the 50 smallest eigenvectors of each horizontal band of data set. The output alpha images for each horizontal band were combined as shown in Figure 10c. Each pixel in this image shows the probability of belonging to the foreground that is water body or the background. The α values in this image range from 0 (water) to 1 (background).

A three-dimensional view of the α values can be seen in Figure 11 that shows a steep change along the bank of the river. As explained earlier, the α value is interpreted as the probability of a pixel to belong to either the foreground or the background.

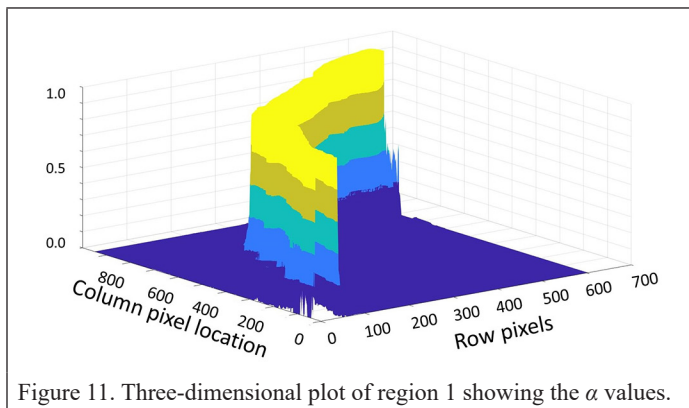


Figure 11. Three-dimensional plot of region 1 showing the α values.

A contour plot was created as shown in Figure 10d at every 0.1 increase in alpha value. Very few contour lines cross across the main channel of the river. This showed that the value of $\alpha < 0.8$ was related to more suitable bank lines. It was observed by visual comparison that a value of $\alpha = 0.5$ resulted in continuous bank lines that closely

aligned with the visible bank line on the original orthoimage. These lines were refined by using smooth line tool available in the ArcMAP toolbox with a the Polynomial Approximation with Exponential Kernel (PAEK) algorithm and were compared to the manually digitized and vendor-provided bank lines for accuracy assessment. The results obtained are discussed in the next section.

Results and Discussion

Two zoomed-in locations are shown in Figure 12 to show the positive and negative findings of the proposed method. The bank lines extracted using the proposed method and the river centerline are shown over the orthoimages.

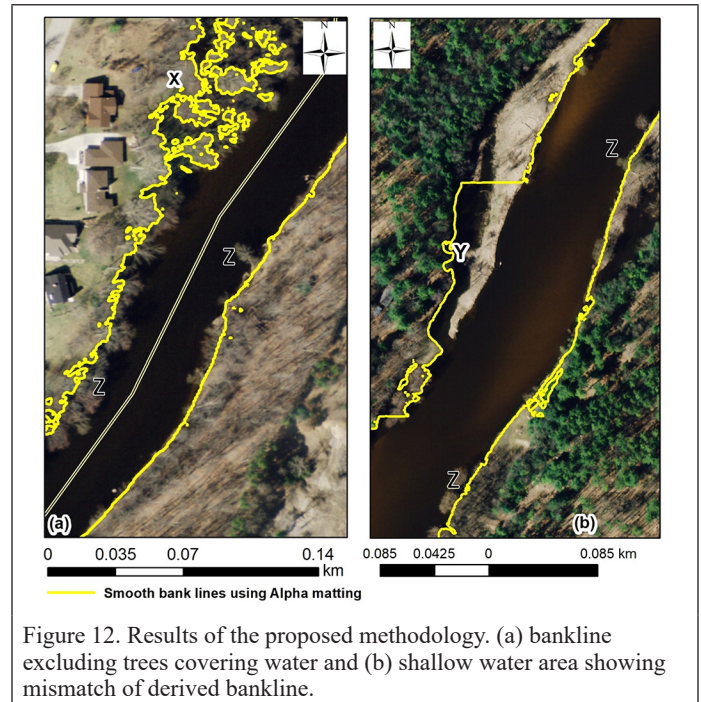


Figure 12. Results of the proposed methodology. (a) bankline excluding trees covering water and (b) shallow water area showing mismatch of derived bankline.

A close visual inspection of the results shows that the bank lines are closely aligned with the visible bank line on the orthoimage. In areas where the banks are covered by the trees (Figure 12, area Z), the line closely follows the trend of the bank. Area X in Figure 12a shows that the proposed method was able to effectively delineate shallow flooding areas along the banks that was not captured by the vendor's bank lines.

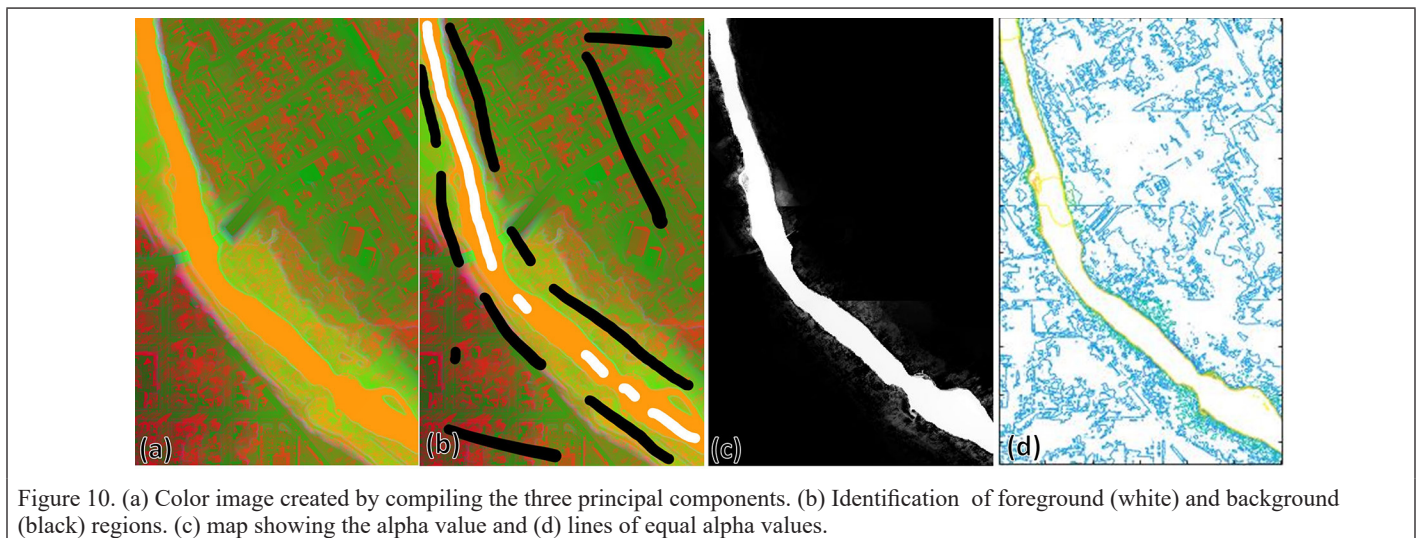


Figure 10. (a) Color image created by compiling the three principal components. (b) Identification of foreground (white) and background (black) regions. (c) map showing the alpha value and (d) lines of equal alpha values.

The drawback of this method is noted in area Y of Figure 12b. It can be noticed that a bank line was not captured because the background scribble was not present in this area. Thus, it was observed that this method was sensitive to the scribble areas identified earlier in the process.

The bank lines were manually digitized using the orthoimage alone. Best visual judgement based on visible water within gaps of trees and meandering pattern of the river was made while digitizing the bank areas covered by trees. Transsects were placed perpendicular to the river centerline at every 30 m, and its intersection with the manually digitized and vendor-provided bank lines, as well as the bank lines produced by the proposed method were determined to calculate the separation. Table 2 summarizes the difference between the three sets of lines. The horizontal differences in areas X and Y and their resultant direction (R) are presented in this table.

Table 2. Statistical comparison of manually digitized, vendor-provided, and alpha matting-based bank lines.

Compared Value	Difference between Manual, Vendor-Provided, and Alpha Matting-Based Bank Lines					
	Absolute (Manual-Vendor)			Absolute (Manual-Alpha Matting)		
	X (m)	Y (m)	R (m)	X (m)	Y (m)	R (m)
Region 1						
Average	1.068	0.567	1.277	0.829	0.413	0.979
Standard deviation	1.204	0.720	1.342	1.110	0.635	1.238
Maximum	8.385	5.428	9.988	6.698	5.223	8.493
Minimum	0.005	0.002	0.007	0.001	0.001	0.002
Region 2						
Average	2.182	1.886	3.244	0.814	1.057	1.506
Standard deviation	2.910	2.925	3.847	1.189	2.612	2.783
Maximum	25.425	20.282	25.533	8.212	21.712	22.699
Minimum	0.020	0.009	0.044	0.000	0.003	0.006

An absolute average separation of 0.98 and 1.5 m was observed for regions 1 and 2, respectively, by comparing the bank lines of the proposed method to the manually digitized lines. The lower average separation observed in region 1 could be attributed to the fact that this region was semiurban, with fewer trees along the bank, whereas the banks in region 2 were covered with dense trees in certain locations. The vendor's bank lines compared poorly to the ones obtained using the presented method. All three methods showed less than a centimeter of minimum separations between each other. The bank lines regions that were unobstructed by trees resulted in the bank lines being close to each other in such areas. Few sections of the two regions were similar to area X in Figure 12a. The maximum separation values were found in areas where the bank lines from the proposed method were significantly away from the vendor's and manual bank lines.

Conclusions

Rivers are most likely covered by vegetation along their bank lines, which makes bank line extraction using only orthoimages a difficult task. Elevation information from lidar provides the extent of the water surface. The complexity of mapping riverbank lines requires use of both the orthoimages and lidar. This paper presents an approach to the delineate riverbank lines by integration of lidar DEM and orthoimages. The methodology was tested at two sites: semiurban and rural to prove its effectiveness. The results show that the influence of the vegetation cover can be minimized using lidar, and the sharp-contrast riverbank from orthoimages can be extracted using the proposed method using alpha matting processes.

During this investigation, several avenues for future study were considered, including the use of other geospatial data sets such as high-resolution satellite images, synthetic aperture radar (SAR), and UAV-based images to improve results. At present, the proposed method requires the identification of foreground and background regions. The

results obtained were sensitive to the selection of background and foreground pixels as explained in "Results and Discussion." Future studies can experiment with the use of methods that classify the foreground and background effectively. The entire process can be improved into an automatic procedure that will locate the bank lines efficiently.

Bank lines for different α values were extracted, and a value of $\alpha = 0.5$ was adopted in this study based on visual inspection of results. Bank lines are very challenging features to extract from lidar or orthoimagery due to their complexity. Further research can be carried out to determine this value based on orthoimages and lidar parameters.

Acknowledgments

We thank the geographic information systems department at Mecosta County, MI, State of Michigan Department of Technology, Management & Budget (DTMB) and the Sanborn Mapping Company for providing the lidar data. The MATLAB code from the paper Levin *et al.* (2008) was modified and used in this study.

References

- Backes, D., M. Smigaj, M. Schimka, V. Zahs, A. Grznárová and M. Scaioni. 2020. River morphology monitoring of a small-scale alpine riverbed using drone photogrammetry and lidar. *International Archives of the Photogrammetry, Remote Sensing and Spatial Information Sciences* 43:1017–1024.
- BhavanGowda, N., J. Manoj, M. H. Mithun, A.R.M. Varma and S. Thota. 2021. Coastline and river banks erosion prediction using image processing. *International Journal of Advanced Research in Computer Science* 12:61–64.
- Cal, A. 2020. High-resolution object-based building extraction using PCA of LiDAR nDSM and aerial photos. In *Spatial Variability in Environmental Science-Patterns, Processes, and Analyses*. London: IntechOpen.
- Chen, L. C., T. A. Teo, Y. C. Shao, Y. C. Lai and J. Y. Rau. 2004. Fusion of LIDAR data and optical imagery for building modeling. *International Archives of Photogrammetry and Remote Sensing* 35(B4):732–737.
- Choung, Y. 2014. Mapping levees using LiDAR data and multispectral orthoimages in the Nakdong River basins, South Korea. *Remote Sensing* 6(9):8696–8717. <https://doi.org/10.3390/rs6098696>.
- Deshpande, S. S. 2013. Improved floodplain delineation method using high-density LiDAR data. *Computer-Aided Civil and Infrastructure Engineering* 28(1):68–79.
- Deshpande, S. S. 2017. *Semi-automated methods to create a hydro-flattened DEM using single photon and linear mode LiDAR points*. Ph.D. dissertation, The Ohio State University, Columbus, OH 145p.
- Deshpande, S. S. and A. Yilmaz. 2017. A semi-automated method to create a lidar-based hydro-flattened DEM. *International Journal of Remote Sensing* 38(5):1365–1387.
- Duró, G., A. Crosato, M. G. Kleinhans and W. S. Uijttewaal. 2018. Bank erosion processes measured with UAV-SfM along complex banklines of a straight mid-sized river reach. *Earth Surface Dynamics* 6(4):933–953.
- Fernández, T., J. L. Pérez-García, J. M. Gómez-López, J. Cardenal, J. Calero, M. Sánchez-Gómez, J. Delgado and J. Tovar-Pescador. 2020. Multitemporal analysis of gully erosion in olive groves by means of digital elevation models obtained with aerial photogrammetric and LiDAR data. *ISPRS International Journal of Geo-Information* 9(4):260.
- Gastal, E.S. and M. M. Oliveira. 2010. Shared sampling for real-time alpha matting. *Computer Graphics Forum* 29(2):575–584.
- Grady, L., T. Schiwietz, S. Aharon and R. Westermann. 2005. Random walks for interactive alpha-matting. *Proceedings of the 5th IASTED International Conference on Visualization, Imaging, and Image Processing*, 7–9 September 2005, Benidorm, Spain, pp. 423–429.
- Grau, J., K. Liang, J. Ogilvie, P. Arp, S. Li, B. Robertson and F. R. Meng. 2021. Using unmanned aerial vehicle and LiDAR-derived DEMs to estimate channels of small tributary streams. *Remote Sensing* 13(17):3380.
- Hamshaw, S. D., T. Engel, D. M. Rizzo, J. O'Neil-Dunne and M. M. Dewoolkar. 2019. Application of unmanned aircraft system (UAS) for monitoring bank erosion along river corridors. *Geomatics, Natural Hazards and Risk* 10(1):1285–1305.

- He, K., C. Rhemann, C. Rother, X. Tang and J. Sun. 2011. A global sampling method for alpha matting. *Conference on Computer Vision and Pattern Recognition*, 20–25 June 2011, Colorado Springs, Colorado, pp. 2049–2056.
- Höfle, B., M. Vetter, N. Pfeifer, G. Mandlbürger and J. Stötter. 2009. Water surface mapping from airborne laser scanning using signal intensity and elevation data. *Earth Surface Processes and Landforms* 34(12):1635–1649.
- Jayathunga, S., T. Owari and S. Tsuyuki. 2018. Analysis of forest structural complexity using airborne LiDAR data and aerial photography in a mixed conifer–broadleaf forest in northern Japan. *Journal of Forestry Research* 29(2):479–493.
- Kummu, M., H. De Moel, P. J. Ward and O. Varis. 2011. How close do we live to water? A global analysis of population distance to freshwater bodies. *Public Library of Science One* 6(6):e20578.
- Legleiter, C. J. 2012. Remote measurement of river morphology via fusion of LiDAR topography and spectrally based bathymetry. *Earth Surface Processes and Landforms* 37(5):499–518.
- Levin, A., A. Rav-Acha and D. Lischinski. 2008. Spectral matting. *IEEE Transactions on Pattern Analysis and Machine Intelligence* 30(10):1699–1712.
- Li, R., S. Deshpande, X. Niu, F. Zhou, K. Di and B. Wu. 2008. Geometric integration of aerial and high-resolution satellite imagery and application in shoreline mapping. *Marine Geodesy* 31(3):143–159.
- Liu, J. K., R. Li, S. Deshpande, X. Niu and T. Y. Shih. 2009. Estimation of blufflines using topographic LiDAR data and orthoimages. *Photogrammetric Engineering & Remote Sensing* 75(1):69–79.
- Mason, J. and D. Mohrig. 2018. Using time-lapse lidar to quantify river bend evolution on the meandering coastal Trinity River, Texas, USA. *Journal of Geophysical Research: Earth Surface* 123(5):1133–1144.
- Myers, D. T., R. R. Rediske and J. N. McNair. 2019. Measuring streambank erosion: A comparison of erosion pins, total station, and terrestrial laser scanner. *Water* 11(9):1846.
- Ngadiman, N., N. M. Kasan, F. H. Hamzan and S.F.S. Zakaria. 2021. Riverbank slope erosion monitoring using unmanned aerial vehicle (UAV). *Multidisciplinary Applied Research and Innovation* 2(1):13–24.
- Niculiță, M., M. C. Mărgărint and P. Tarolli. 2020. Using UAV and LiDAR data for gully geomorphic changes monitoring. *Developments in Earth Surface Processes* 23:271–315.
- Rhemann, C., C. Rother and M. Gelautz. 2008. Improving color modeling for alpha matting. *Proceedings of the British Machine Vision Conference*, 1–4 September 2008, Leeds, England, United Kingdom.
- Rinaldi, M., S. Dufour, W. Bertoldi and A. Gurnell. 2013. River processes and implications for fluvial ecogeomorphology: A European perspective. In *Treatise on Geomorphology: Volume 12. Ecogeomorphology*, edited by J. Shroder, D. R. Butler, and C. R. Hupp. San Diego: Academic Press, pp. 37–52.
- U.S. Geological Survey. 2024. Lidar Base Specification Appendix 2: Hydro-flattening Reference. <<https://www.usgs.gov/ngp-standards-and-specifications/lidar-base-specification-appendix-2-hydro-flattening-reference>> (last date access: 15 August 2024 month year).
- Vandromme, R., A. Foucher, O. Cerdan and S. Salvador-Blanes. 2017. Quantification of bank erosion of artificial drainage networks using LIDAR data. *Zeitschrift für Geomorphologie* 61(1):1–10.
- Wolter, C. F., K. E. Schilling and J. A. Palmer. 2021. Quantifying the extent of eroding streambanks in Iowa. *Journal of the American Water Resources Association* 57(3):391–405.

SUSTAINING MEMBERS

Applanix

Richmond Hill, Ontario, Canada
<http://www.applanix.com>
 Member Since: 7/1997

Ayres Associates

Madison, Wisconsin
www.AyresAssociates.com
 Member Since: 1/1953

Dewberry

Fairfax, Virginia
www.dewberry.com
 Member Since: 1/1985

Digital Mapping, Inc.(DMI)

Huntington Beach, California
www.admap.com
 Member Since: 4/2002

Environmental Research Incorporated

Linden, Virginia
www.eri.us.com
 Member Since: 8/2008

Esri

Redlands, California
www.esri.com
 Member Since: 1/1987

GeoCue Group

Madison, Alabama
<http://www.geocue.com>
 Member Since: 10/2003

GeoDyn GmbH

Munich, Germany
www.geodyn.com/index
 Member Since: 3/2024

Geographic Imperatives LLC

Centennial, Colorado
 Member Since: 12/2020

GPD Group

Columbus, Ohio
<https://gpdgroup.com/>
 Member Since: 7/2024

GPI Geospatial Inc.

Orlando, Florida
www.aca-net.com
 Member Since: 1/1994

Keystone Aerial Surveys, Inc.

Philadelphia, Pennsylvania
www.kasurveys.com
 Member Since: 1/1985

Kucera International

Willoughby, Ohio
www.kucerainternational.com
 Member Since: 1/1992

L3Harris Technologies

Broomfield, Colorado
www.l3harris.com
 Member Since: 6/2008

Merrick & Company

Greenwood Village, Colorado
www.merrick.com
 Member Since: 4/1995

Miller Creek Associates

SeaTac Washington
www.mcamaps.com
 Member Since: 12/2014

NV5 Geospatial

Sheboygan Falls, Wisconsin
www.quantumspatial.com
 Member Since: 1/1974

Pickett and Associates, Inc.

Bartow, Florida
www.pickettusa.com
 Member Since: 4/2007

PixElement

Belmont, Michigan
<https://pixelement.com>
 Member Since: 2/2017

Riegl USA, Inc.

Orlando, Florida
www.rieglusa.com
 Member Since: 11/2004

Sanborn Map Company

Colorado Springs, Colorado
www.sanborn.com
 Member Since: 10/1984

Surdex Corporation

(a Bowman company)
 Chesterfield, Missouri
www.surdex.com
 Member Since: 12/2011

Surveying And Mapping, LLC (SAM)

Austin, Texas
www.sam.biz
 Member Since: 12/2005

T3 Global Strategies, Inc.

Bridgeville, Pennsylvania
<https://t3gs.com/>
 Member Since: 6/2020

Towill, Inc.

San Francisco, California
www.towill.com
 Member Since: 1/1952

Woolpert LLP

Dayton, Ohio
www.woolpert.com
 Member Since: 1/1985

SUSTAINING MEMBER BENEFITS

Membership

- ✓ Provides a means for dissemination of new information
- ✓ Encourages an exchange of ideas and communication
- ✓ Offers prime exposure for companies

Benefits of an ASPRS Membership

- Complimentary and discounted Employee Membership*
- E-mail blast to full ASPRS membership*
- Professional Certification Application fee discount for any employee
- Member price for ASPRS publications
- Discount on group registration to ASPRS virtual conferences
- Sustaining Member company listing in ASPRS directory/website
- Hot link to company website from Sustaining Member company listing page on ASPRS website
- Press Release Priority Listing in PE&RS Industry News
- Priority publishing of Highlight Articles in PE&RS plus, 20% discount off cover fee
- Discount on PE&RS advertising
- Exhibit discounts at ASPRS sponsored conferences (exception ASPRS/ILMF)
- Free training webinar registrations per year*
- Discount on additional training webinar registrations for employees
- Discount for each new SMC member brought on board (Discount for first year only)

PUBLISHING OPEN-ACCESS IN *PE&RS* IS NOW EASIER!

ASPRS has changed the subscription model of our monthly journal, *PE&RS*. ASPRS is waiving open-access fees for primary authors from subscribing institutions. Additionally, primary authors who are Individual Members of ASPRS will be able to publish one open-access article per year at no cost and will receive a 50% discount on open-access fees for additional articles.

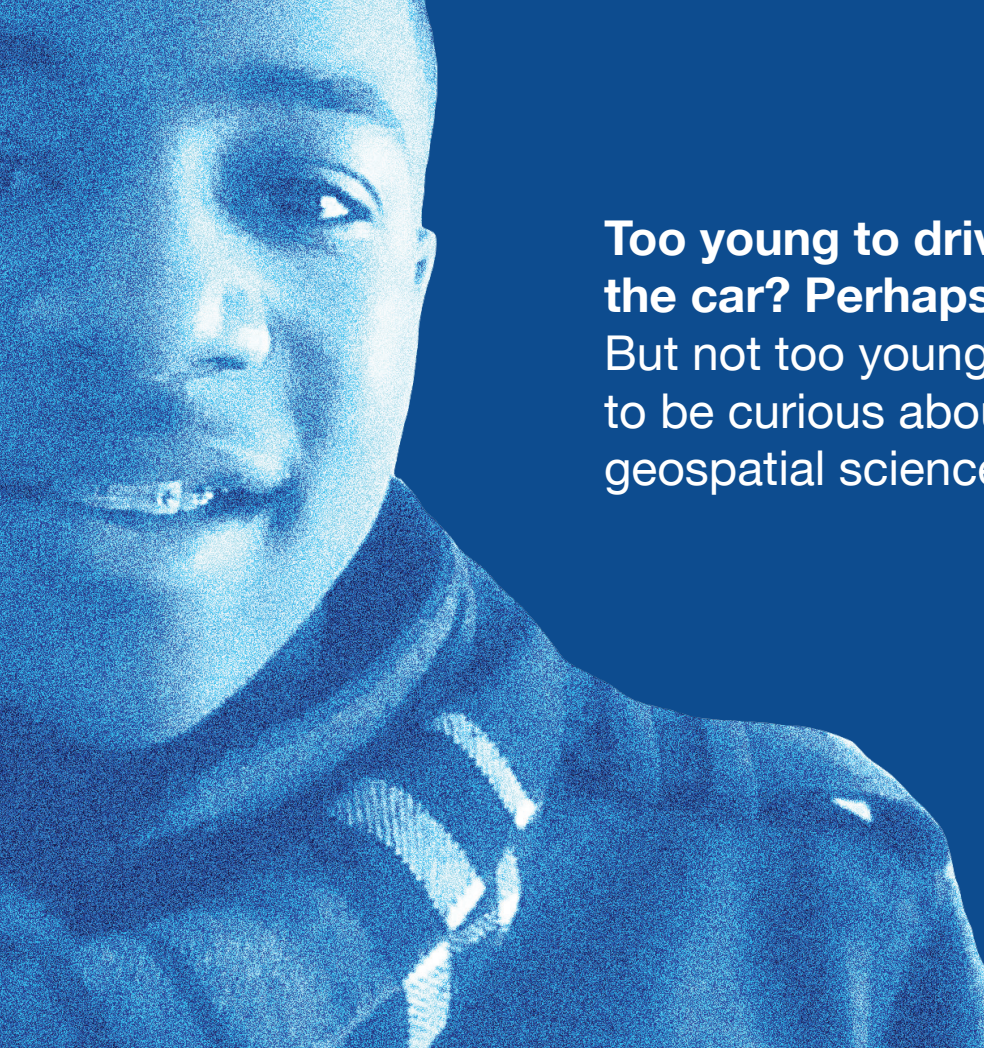


- **Open Access matters!** By providing unrestricted access to research we can advance the geospatial industry and provide research that is available to everyone.
- **Institutions and authors receive more recognition!** Giving permission to everyone to read, share, reuse the research without asking for permission, as long as the author is credited.
- **Reputation matters!** Known for its high standards, *PE&RS* is the industry leading peer-review journal. Adding open access increases authors' visibility and reputation for quality research.
- **Fostering the geospatial industry!** Open access allows for sharing without restriction. Research is freely available to everyone without an embargo period.

Under the previous subscription model, authors and institutions paid \$1500 or more in open-access fees per article. This will represent a significant cost savings. Open-access publications benefit authors through greater visibility of their work and conformance with open science mandates of funding agencies.

Subscriptions asprs.org/subscribe
Membership asprs.org/membership





**Too young to drive
the car? Perhaps!**
But not too young
to be curious about
geospatial sciences.



**The ASPRS Foundation
was established to advance
the understanding and
use of spatial data for the
betterment of humankind.**

*The Foundation provides grants,
scholarships, loans and other forms of aid
to individuals or organizations pursuing
knowledge of imaging and geospatial
information science and technology, and
their applications across the scientific,
governmental, and commercial sectors.*

**Support the foundation, so when
they are ready, we are too.**

asprsfoundation.org/donate

JOIN ASPRS TODAY!



asprs THE IMAGING & GEOSPATIAL
INFORMATION SOCIETY

ACCELERATE YOUR CAREER!

PHOTOGRAMMETRY · REMOTE SENSING · GIS · LIDAR · UAS ...and more!

LEARN

- Read our journal, *PE&RS*
- Attend professional development workshops, GeoBytes, and online courses through the ASPRS ProLearn platform
- Earn professional development hours (PDH)
- Attend our national & regional meetings and conferences

DO

- Write for *PE&RS*
- Innovate to create new geospatial technologies
- Present at our national & regional meetings and conferences
- Engage & network

GIVE

- Participate in the development of standards & best practices
- Influence state licensure through our NCEES affiliation
- Mentor colleagues & support students
- Educate others about geospatial science & technology

BELONG

- Establish yourself as a geospatial expert
- Grow business relationships
- Brand yourself and your company as geospatial leaders
- Connect to the world via our affiliation with ISPRS

Don't delay, join today at **asprs.org**